



HAL
open science

Source rocks in foreland basins: a preferential context for the development of natural hydraulic fractures

Alain Zanella, Peter R Cobbold, Nuno Rodrigues, H Loseth, Marc Jolivet, F
Gouttefangeas, D Chew

► To cite this version:

Alain Zanella, Peter R Cobbold, Nuno Rodrigues, H Loseth, Marc Jolivet, et al.. Source rocks in foreland basins: a preferential context for the development of natural hydraulic fractures. AAPG Bulletin, 2021, 105 (4), pp.647-668. 10.1306/08122018162 . insu-03010282

HAL Id: insu-03010282

<https://insu.hal.science/insu-03010282v1>

Submitted on 17 Nov 2020

HAL is a multi-disciplinary open access archive for the deposit and dissemination of scientific research documents, whether they are published or not. The documents may come from teaching and research institutions in France or abroad, or from public or private research centers.

L'archive ouverte pluridisciplinaire **HAL**, est destinée au dépôt et à la diffusion de documents scientifiques de niveau recherche, publiés ou non, émanant des établissements d'enseignement et de recherche français ou étrangers, des laboratoires publics ou privés.



Source rocks in foreland basins: a preferential context for the development of natural hydraulic fractures.

A. Zanella, P.R. Cobbold, N. Rodrigues, H. Loseth, M. Jolivet, F. Gouttefangeas, and D. Chew

AAPG Bulletin published online 28 August 2020
doi: 10.1306/08122018162

Disclaimer: The AAPG Bulletin Ahead of Print program provides readers with the earliest possible access to articles that have been peer-reviewed and accepted for publication. These articles have not been copyedited and are posted “as is,” and do not reflect AAPG editorial changes. Once the accepted manuscript appears in the Ahead of Print area, it will be prepared for print and online publication, which includes copyediting, typesetting, proofreading, and author review. ***This process will likely lead to differences between the accepted manuscript and the final, printed version.*** Manuscripts will remain in the Ahead of Print area until the final, typeset articles are printed. Supplemental material intended, and accepted, for publication is not posted until publication of the final, typeset article.

Cite as: Zanella, A., P.R. Cobbold, N. Rodrigues, H. Loseth, M. Jolivet, F. Gouttefangeas, and D. Chew, **Source rocks in foreland basins: a preferential context for the development of natural hydraulic fractures.**, (*in press; preliminary version published online Ahead of Print 28 August 2020*): AAPG Bulletin, doi: 10.1306/08122018162.

1 Source rocks in foreland basins: a preferential context for the 2 development of natural hydraulic fractures.

3
4 A. Zanella^{a*}, P.R. Cobbold^b, N. Rodrigues^{b,c}, H. Loseth^c, M. Jolivet^b, F. Gouttefangeas^d, D.
5 Chew^e

6
7 ^a*Le Mans Université, L.P.G-UMR 6112, avenue Olivier Messiaen, 72085 Le Mans, Cedex 9, France*

8 ^b*Géosciences Rennes, UMR 6118, Université de Rennes 1, 35042 Rennes, France*

9 ^c*Statoil Research Centre, 7005 Trondheim, Norway*

10 ^d*Centre de Microscopie Electronique à Balayage et Microanalyse, Université de Rennes 1, 35042 Rennes, France*

11 ^e*Department of Geology, Trinity College Dublin, Dublin 2, Ireland*

12 ^{*}*Corresponding author: alain.zanella@univ-lemans.fr*

13 14 KEYWORDS

15 beef veins; natural hydraulic fractures; petroleum source rocks; fluid overpressure; foreland basins

16 17 ABSTRACT

18
19 Bedding-parallel veins of fibrous calcite (also called BPV or ‘beef’) occur in many sedimentary
20 basins, especially those containing low-permeability strata with organic source material for petroleum.
21 The formation of such veins is often linked with fluid overpressure in these source rocks. In this
22 review, we demonstrate that beef veins are most commonly present in foreland basins worldwide or in
23 basins that recorded a compressive tectonic period. The formation of beef veins is related to two main
24 phases: (1) the initiation of bedding-parallel fracture and (2) the infilling of the fracture.

25 Previous structural studies have shown that formation of beef veins occurred during a period of
26 compressive stress activity. This is especially the case for the Wessex Basin (UK) and the Neuquén
27 Basin (Argentina). Here we provide more observations for other basins: the Cordillera Oriental
28 (Colombia), the Paris Basin (France), the northern Pyrenees (France), the Uinta Basin (US), the Tian
29 Shan Mountains (central Asia) and the Appalachian Mountains (US). In the Paris Basin, beef vein
30 formation is dated at 155 Ma (U/Pb calcite method) and is coeval with the compressional deformation
31 in the eastern part of the basin.

32 Because of the timing of generation for such veins and even if the theory and the experiments of
33 fracturing demonstrate that bedding-parallel fractures can be generated only with a distributed fluid
34 overpressure, the formation of beef veins seems to be a consequence of both fluid overpressures and a
35 compressional tectonic stress.

36

37

38 **1. Introduction**

39

40 Many of the major mountain ranges around the world have resulted from recent horizontal
41 shortening and vertical thickening (Figure 1). Others have resulted from rifting, strike-slip faulting or
42 uplift associated with magmatism. In contrast, most older mountain ranges have tended to disappear
43 by active erosion of their sharp topographic profiles. For recent shortening and thickening, the main
44 causes are (1) subduction beneath active continental margins, especially in the Atlantic and Pacific
45 oceans, or (2) continental collision, for example between Europe and Africa or central Asia and India
46 (Figure 1). In such tectonic settings, there has been progressive development of adjacent foreland
47 basin systems as a result of thrusting and local sedimentation and in many cases, they contain
48 petroleum systems.

49 Because they are commonly hydrocarbon-bearing, foreland basins are major targets for the
50 study of source rocks and reservoirs. In the last twenty years, organic-rich source rocks have been
51 extensively studied because of their hydrocarbon potential. Within these sedimentary units, many
52 fractures occur and some of them can affect the permeability as well as the cap capability of the source
53 rocks. This is especially the case for the natural hydraulic fractures, such as bedding-parallel veins
54 (also called BPV or 'beef'). The first examples of beef to be described were likely those in the Wessex
55 Basin of Southern England (Buckland & De la Beche, 1835). The veins were easily observable along
56 coastal cliffs and provided useful material for building walls and roads. More generally, bedding-
57 parallel veins are common worldwide in sedimentary basins, especially those containing
58 hydrocarbons, indicating that the host rock has reached maturity (Cobbold et al., 2013; Gale et al.,
59 2014). The formation of such veins is often linked to fluid overpressure during hydrocarbon generation
60 (Rodrigues et al., 2009; Zanella et al., 2015a). Beef veins therefore consist of natural hydraulic
61 fractures, infilled by a fibrous mineral, such as calcite, gypsum or quartz (Cobbold et al. 2013). Other
62 mechanisms are also involved, but seem to be more minor, such as, for example, the force of
63 crystallization (e.g. Taber, 1916; Means & Li, 2001; Gratier et al., 2012). Recent studies have shown
64 that many bedding-parallel veins formed during horizontal shortening, as in the Wessex Basin,
65 southern England, (Zanella et al., 2015b), in the Bristol Channel Basin, England and Wales, (Meng et
66 al., 2017), or in the Neuquén Basin of western Argentina (Rodrigues et al., 2009; Ukar et al., 2017;
67 Ukar et al. 2018).

68 This paper presents a worldwide review of bedding-parallel veins (natural hydraulic fractures)
69 within foreland basins and discusses the development of such natural hydraulic fracturing processes
70 within this particular tectonic basin setting. We also present new observations and data to complete
71 those of previous studies, particularly with respect to four localities: (1) the Northern Pyrenees,
72 France; (2) the Uinta Basin, USA; (3) the Tian Shan Basin, China and (4) the Appalachian Basin,
73 USA.

74

75

76 **2. Formation of beef veins**

77

78 The simplest calcite beef veins, which form in tectonically quiescent basins, are typically bedding-
79 parallel (horizontal), of regular thickness and contain calcite fibers, which have formed almost
80 vertically and antitaxially, separating the two boundaries of the fracture. The best evidence for
81 epitaxial separation comes from the presence of flattened fossils (for example, ammonites), which
82 remain in the central part of the vein, while counterparts of them are visible at the two outer
83 boundaries, but displaced along the directions of the calcite fibers, which may be somewhat oblique
84 (Rodrigues et al., 2009). Other forms of calcite beef are cone-in-cone structures, which likely form as a
85 result of shear faulting during epitaxial growth of the calcite veins (e.g. Cobbold et al. 2013).

86 Two successive phases characterize the formation of a beef vein: (1) the initiation of the fracture
87 and (2) the opening of the fracture. For the initiation of the fracture, the model can explain the
88 generation of horizontal hydraulic fractures without external tectonic stresses (e.g. compressive stress)
89 (Cobbold et al. 2007, Mourgues & Cobbold, 2003). However, much of our knowledge of the
90 mechanisms involved in such processes come from experimental models developed during the early
91 21st century. In the early iterations of these experimental models, the pore fluids were injected from the
92 outside, at measured rates and pressures (Cobbold & Castro, 1999; Mourgues & Cobbold, 2003).
93 Thus, it became clear that vertical gradients of overpressure counteract the weight of the granular
94 material. When noncohesive materials were also compressed horizontally, the pore fluid gradient
95 facilitated detachments for thrust faults and caused these to become more nearly horizontal (Cobbold
96 et al., 2001). When the material was cohesive, the vertical pressure gradient generated horizontal
97 tensile fractures, which opened progressively (Cobbold & Rodrigues, 2007). Moreover, when the
98 models were also compressed horizontally, the resulting stresses facilitated the formation of horizontal
99 tensile fractures. Because the early experimental models simulated the origin of the fluid overpressure
100 as an injector-type system, they were not adapted for the study of the origin and mechanisms involved
101 in the development of such fluid overpressures.

102 Thus, to be able to study the origin of fluid overpressures and the parameters involved in the
103 process of natural hydraulic fracturing within source rocks, later experiments have used transition
104 phases (solid to liquid), to produce a fluid within a closed experimental setup. From solid organic
105 particles (such as beeswax microspheres), models were able to generate a fluid by chemical
106 compaction-like mechanisms, which occur during burial of organic-rich source rock (Fig. 2;
107 Lemrabott & Cobbold, 2010; Zanella et al., 2014a). In such models, the wax was able to melt, on
108 heating the model from below. The resulting decrease in underlying support allowed solid particles to
109 move downwards, causing compaction of the underlying framework and an increase in pore fluid

110 pressure, by a mechanism of load transfer (Zanella et al. 2014a). In other models, which were saturated
111 with water but not subject to horizontal shortening (Figure 2), the overpressure developed soon after
112 the temperature had reached the melting point of beeswax, at the base of the model. This overpressure
113 became great enough to cause horizontal hydraulic fracturing of the wax-rich layer. Molten wax then
114 migrated vertically and horizontally through the pore space and filled the opening generated by
115 hydraulic fractures. In similar models, which were also subject to horizontal shortening, the hydraulic
116 fractures developed more strongly, becoming wider and longer. Furthermore, many of the fractures
117 varied laterally in thickness and orientation, as a result of local folding and thrust faulting.
118

119 For the filling of the natural hydraulic fractures, beef veins appear to have incrementally grown
120 by successive phases of crystallization (e.g. Taber, 1918; Ramsay, 1980; Rodrigues et al., 2009). Thus,
121 fibers appear to have grown incrementally during the displacement of the edges of the veins by a
122 crack-seal mechanism (Ramsay, 1980) or more continuously (Taber 1918; Durney & Ramsey, 1973;
123 Means & Li, 2001). The mechanisms involved in the formation of beef veins are complex and several
124 of them have been postulated by previous authors. The opening of the vein implies a key mechanism
125 already describe by several authors: the force of crystallization (e.g. Baker et al., 2006; Bons, 2001;
126 Bons et al., 2012; Keulen et al., 2001; Mean & Li, 2001). Indeed, several experiments have
127 demonstrated the great importance of the force of crystallization in the beef vein opening (Bons &
128 Jessel, 1997; Hilgers et al., 2001; Nollet et al., 2005, 2009) Thus, the tectonic stress, the pore fluid
129 pressure (fluid overpressures) and the force of crystallization appear to be the major mechanisms (e.g.
130 Sibson, 2003; Shearman et al., 1972; Stoneley, 1983; Taber, 1916; Gratier et al., 2012).
131

132 In many basins worldwide, the formation of beef veins seems to be linked to the generation of
133 hydrocarbons, as showing by scanning electron microscopy for calcite beef of the Wessex Basin
134 (Zanella et al., 2015b), the Neuquén Basin (Rodrigues et al., 2009; Ukar et al. 2017, 2018), the
135 Magellan Basin (Zanella et al., 2014b) and the Paris Basin. All of these examples show that beef veins
136 contain inclusions of organic matter (liquid, solid or both) within or next to the calcite crystals,
137 indicating that the organic matter was diffusing, while the calcite crystals were growing. Other
138 examples of calcite beef, e.g. in the Lourdes area, the Uinta Basin or the Appalachians, may either
139 include or be adjacent to veins of organic material. Investigating the relationship between the organic
140 matter and the hydraulic fracturing, Zanella et al. (2014a) showed with their experiments that the
141 maturity degree is a key parameter to explain the increase of pore fluid pressure within source rocks
142 and that a horizontal compressive stress can favor the development of horizontal hydraulic fractures.
143
144

145 **3. Worldwide distribution of beef veins within foreland basins**

146

147 *3.1. Foreland basins*

148

149 A global topographic map (Figure 1) illustrates the occurrence of significant present-day
150 mountain ranges, especially along continental margins such as the Andes or within zones of
151 continental collision (such as central Asia or the Alps). Many recent foreland basins have formed next
152 to these current mountain ranges. Additional evidence for compressional reactivation of such
153 mountains comes from stress maps on a global scale, which show directions of horizontal
154 compressional stress (e.g. Heidbach et al., 2009). Although many such mountain ranges have formed
155 recently and expose Mesozoic or younger rocks, others expose older rocks (Paleozoic or even
156 Precambrian). In many cases, however, older mountain belts have been subject to recent localized
157 reactivation, such as the Appalachian Mountains in the eastern US and Canada, but also parts of the
158 mountains of Scotland, Norway, Brazil, northern Africa or Australia. Indeed, such reactivation
159 explains why the mountains still exist today, despite relatively active erosion.

160 Foreland basins (such as those next to the Andes) tend to have relatively low and flat upper
161 surfaces, but deep basements, which have subsided, as a result of (1) the weight of nearby mountains,
162 (2) the propagation of outward-verging thrust faults, (3) the local accumulation of sediments derived
163 from erosion of the mountains, (4) the accumulation of evaporites or limestones within local
164 depressions and (5) the accumulation of volcanic and plutonic rocks propagated out from the mountain
165 belt, especially in subduction zone settings.

166 Petroleum source rocks (commonly of Mesozoic age, but also of Paleozoic age) often have
167 formed within many of these foreland basins, in part because the surface depressions yield sufficient
168 accommodation space, but also because of suitable climatic and environmental conditions. Progressive
169 subsidence of foreland basins leads to heating and maturation of source rocks at depth. Fluid
170 overpressure tends to be common within such source rocks, as a result of the heating, maturation,
171 increases in volume and chemical compaction (under the weight of the overlying rock column and the
172 effect of horizontal tectonic compression). Such heating is mainly associated with burial but may also
173 be due to magmatic intrusions, especially in subduction zone systems (Zanella et al. 2015a).

174 Finally, thrust detachments are common in foreland basins, especially within overpressured
175 source rocks, where seepage forces counteract the weight of gravity and sedimentary strata providing
176 an anisotropic mechanical response (Cobbold et al., 2001).

177

178 *3.2. Calcite beef within foreland basins (Mesozoic host rocks)*

179

180 Calcite beef is common within petroleum source rocks, especially those which have reached
181 maturity (Table. 1). In the last few years, several authors have described examples of beef within
182 foreland basins, especially within Mesozoic rocks of the Wessex Basin (UK), the Neuquén Basin

183 (Argentina), the Magellan Basin (Chile and Argentina) and the Paris Basin (France). Other examples
184 have been described worldwide (e.g. Cobbold et al., 2013; Gale et al. 2014), although not necessarily
185 in such detail.

186 Where a basin has been subject to compressional tectonics, it may also contain synchronous
187 calcite beef. Typically, the veins will then be variable in thickness and orientation (Figs. 3, 4 and 5). A
188 vein may vary in thickness across small amplitude folds becoming thicker within synclines and thinner
189 over anticlines. Other variations in thickness may occur across reverse faults (see the examples from
190 the Wessex Basin; Figure 3). In the Magellan Basin, Zanella et al. (2014b) show that beef vein
191 occurrences are more numerous closed to main thrust faults. Finally, some veins may have formed
192 obliquely to bedding, (i.e. nearly horizontally) after the bedding has rotated, as a result of
193 compressional deformation. These structures are similar to some of those described from the
194 experimental modeling with fluid overpressures (Zanella et al., 2014a).

195

196 3.2.1. Wessex Basin, southern England

197

198 The Wessex Basin covers much of southern England (Figure 3A) and consists of Mesozoic and
199 Cenozoic rocks that young in general towards the east, but is subject to folding and faulting, especially
200 near the southern basin margin (Wight-Bray and Purbeck faults). A north-south section across the
201 Purbeck fault (Figure 3A) and its restoration, published by Underhill & Stoneley (1998), show that
202 much of the slip has been of Late Cretaceous to Cenozoic age. The Wessex Basin also has several
203 oilfields, which produce hydrocarbons from Jurassic source rocks (Underhill & Stoneley, 1998).

204 Within the Liassic source rocks, calcite beef are common and have drawn attention for many
205 years from geologists (e.g. Lang et al., 1923; Richardson, 1923; Buckland & De la Beche, 1835;
206 Marshall, 1982), who at first attributed them to early diagenesis of the sediments. However, later work
207 revealed epitaxial growth of calcite fibers (e.g. Cobbold & Rodrigues, 2007), after splitting of the
208 rock.

209 On studying other calcite veins in the Purbeck Formation (latest Jurassic or Early Cretaceous) at
210 Lulworth Cove (above the Purbeck fault), Zanella et al. (2015b) discovered that many of them are
211 localized very close to thrust faults (Figure 3). These veins show sigmoidal fibers (Fig. 3B & C) as
212 well as variations in thickness around folds (Figure 3D). Such observations argue for a vein
213 development synchronous with a horizontal shortening period. Indeed, recent uranium-lead dating of
214 calcite (Chew et al., work in progress) has produced Albian ages (about 107 Ma) for such
215 compressional beef veins, both at Lulworth Cove and also at Charmouth (in the Shales-with-Beef
216 Formation of Liassic age). Thus, the beef veins in the Wessex Basin formed during the onset of
217 inversion tectonics.

218

219 3.2.2. Neuquén Basin, western Argentina

220

221 The Neuquén Basin covers an area of western Argentina, in the Andean foreland (Figure 4A). Its
222 western margin is in the sub-Andes and it contains many north-northwest-trending folds. An eroded
223 anticline exposes large areas of the Vaca Muerta Formation (Figure 4A), which is an Upper Jurassic
224 organic-rich shale and a world-class source rock for oil. A geological section (Figure 4B, after Vera et
225 al., 2014), through the city of Chos Malal (eastern side of the cross-section on Figure 4B), illustrates
226 uplifted blocks of Palaeozoic basement, as well as thrust faults, many of which have detached near the
227 base of the Vaca Muerta Formation.

228 Also, in the Vaca Muerta Formation are many examples of calcite beef. Although some of these
229 veins are as much as 30 cm thick and are laterally continuous over distances of hundreds of meters
230 (e.g. Cobbold et al., 2013, fig. 3A; Gale et al., 2014), others show local variations in thickness across
231 minor folds and reverse faults (Figure 4A), indicating that they formed during horizontal compression
232 and shortening. By analyses of the domal structures from beef veins, Ukar et al. (2017) concluded that
233 beef veins, in the area of Loncopué, developed during the Late Cretaceous. This conclusion is
234 consistent with Rodrigues (2008) and Weger et al. (2018), which concluded by isotopes analysis that
235 beef veins growth occurred at depth related to high temperatures (120°C to 185°C). Beef veins also
236 occur elsewhere in the Neuquén Province (Cobbold et al., 2013) within shales of the Los Molles
237 Formation (Lower Jurassic) or Agrió Formation (Lower Cretaceous). Finally, beef veins also occur in
238 the Vaca Muerta Formation further north in Mendoza Province (Zanella et al., 2015a).

239 In summary, there is good evidence in the Neuquén Basin for recent overpressure, thrust
240 detachments and multiple veins of compressional calcite beef, all within source-rock shale. Much of
241 the heating was probably related to foreland subsidence, but some may have come from magmatic
242 intrusions, which are abundant, especially in Mendoza Province (Zanella et al., 2015a).

243

244 3.2.3. Edges of the Cordillera Oriental, central Colombia

245

246 The Cordillera Oriental is an Andean mountain belt in eastern part of Colombia (Fig. 5A, after
247 Mora et al., 2015). Within it, folds and thrusts trend north-northeast, affecting mainly Cretaceous
248 rocks. The geological section shows uplift of Paleozoic to Precambrian basement between reverse
249 faults, as well as major folds within Cretaceous sedimentary rocks, some of which are source rocks for
250 petroleum (Figure 5A). On the western side of the Cordillera, folds and thrusts verge towards the west
251 (Figure 5A) and Cretaceous shales contain layers of calcite beef (white to yellow), which vary in
252 thickness across folds (Figure 5C). At the eastern edge of the Cordillera, in the Macanal Formation
253 (Lower Cretaceous), some beef contains thin layers of yellow pyrite, which have folded (Figure 5B,
254 bottom right), while calcite has grown antitaxially above and below them, filling synclines more than
255 anticlines, indicating a synchronous development with a horizontal shortening.

256 In summary, there is good evidence, at both edges of the Cordillera Oriental, for recent
257 overpressure, thrust detachments and multiple veins of compressional calcite beef veins, all within
258 organic-rich mature shale source rocks.

259

260 3.2.4. Paris Basin, northcentral France

261 The Paris Basin occupies a large area of northcentral France (Figure 6A) and consists mainly of
262 Triassic, Jurassic and Cretaceous marine strata, but also some Cenozoic strata (mainly lacustrine) in its
263 central part (Guillocheau et al., 2000). A cross-section (Figure 6A) shows that the basin has undergone
264 some uplift and erosion, especially on its eastern margin. In the past, there have been some
265 descriptions of calcite beef or cone-in-cone structures, mostly within Jurassic shales of the Schistes
266 Carton Formation (lower Toarcian, about 185 Ma) on the eastern basin margin (e.g. Denaeyer, 1943,
267 1947), but also within Callovian shales at the northern edge (Voisin, 1999). The Schistes Carton have
268 been subject to much exploration as potential source rocks for oil, and this has revealed the presence
269 of fluid overpressure at several localities. Cobbold et al. (2015) investigated a ditch through the
270 Schistes Carton Formation at Gélaucourt, near Nancy at the eastern edge of the basin (Fig. 6B, left).
271 The ditch (Figure 6B, left) contains many beef veins, several cm thick and several meters long (Fig.
272 6B, right). These veins had been identified previously by Denaeyer (1947). They consist mainly of
273 calcite fibers, almost perpendicular to bedding, but they also contain some inclusions of hydrocarbons,
274 which are visible in hand specimens, but especially by scanning electron microscopy (Figure 7B;
275 Cobbold et al., 2015). Recently, by uranium-lead dating of calcite, we have determined the age of
276 formation of this calcite beef to be 155 Ma (Figure 7A). This is about 30 m.y. younger than the
277 stratigraphic age of the host rock (about 185 Ma). Indeed, the age of the calcite almost coincides with
278 the age of onset of compressional deformation on the eastern edge of the Paris Basin (see Guillocheau
279 et al., 2000).

280

281 **4. New results: field data for calcite beef in other compressional basins**

282

283 4.1. Lourdes, northern Pyrenees, France (locality 22)

284

285 At the northern edge of the Pyrenees, a major thrust fault zone separates this mountain range to
286 the south from the Aquitaine Basin to the north. Geological maps of Lourdes (e.g. BRGM, Carte
287 Géologique Détaillée de la France, 1:50 000, sheet XVI-46, 1970) show multiple folds and faults
288 within Mesozoic strata, especially near the town of Lourdes (Choukroune, 1969). Indeed, an oblique
289 view of the Pic du Béout hills, to the east of Lourdes (Figure 8A) shows repetitions of resistant white
290 Aptian-Albian limestones, which dip 30° to 40° towards the south. Between the limestones are darker
291 and softer layers of upper Aptian shale, which have acted as thrust detachments and exhibit some

292 cleavage and down-dip lineations. The plains surrounding the hills consist mainly of unconformably
293 overlying Upper Cretaceous flysch. Some of the upper Aptian shale contains layers of fibrous calcite
294 beef (Figure 8B), especially near the village of Aspin-en-Lavedan (Figure 8A). Many of the veins are
295 almost parallel to bedding, whereas younger ones are less steeply dipping and therefore somewhat
296 oblique to bedding. The dipping of the sediments is the result of the compressional deformation from
297 the Late Cretaceous to present day. Because the compression is active since these geological times,
298 beef veins in this area are synchronous with this deformation. Thus, they probably formed once the
299 bedding had rotated and partly as a result of compressional deformation. Our analyses, by scanning
300 electron microscopy (Figure 8C), have revealed steep fractures across a flat-lying vein of calcite beef,
301 the fractures containing much more carbon (orange color) than pure calcite.

302 It also happens that the Aquitaine Basin is hydrocarbon prone, especially beneath low-
303 permeability upper Aptian shale (Biteau & Canérot, 2007). Thus, there is evidence, around Lourdes,
304 for synchronicity of (1) Late Cretaceous or Cenozoic compressional deformation, (2) generation and
305 accumulation of organic-rich fluids and (3) formation of calcite beef.

306

307 4.2. Uinta Basin, Utah (locality 12)

308

309 While investigating the presence of bitumen veins in the Uinta Basin, we discovered veins of
310 calcite beef (up to 3 cm thick), which are common within Eocene shales of the Green River Formation,
311 which are also source rocks for petroleum with several major oil fields. The Uinta Basin is a typical
312 intermontane basin (Fig. 9A). At its northern edge, the basin abuts a major thrust fault, which has
313 uplifted Paleozoic basement (part of the Uinta Mountains). At the northern margin of the basin,
314 overpressure occurs within hydrocarbons of the Altamont-Bluebell oil field (Dubiel, 2003). Elsewhere,
315 exposures of Green River shales (for example, within open mines) contain visible beef, which consist
316 mainly of calcite with dominantly vertical fibers (Fig. 9B). However, in some places the veins consist,
317 not only of calcite, but also of solid hydrocarbons (gilsonite; Fig. 9C). Some veins also contain
318 bitumen between fibers of calcite. Thus, there is evidence for synchronicity of compressional
319 tectonics, maturation of source rocks and growth of beef veins.

320

321 4.3. Tian Shan Mountains, central Asia (localities 30 to 32)

322

323 In central Asia, the Tian Shan Mountains (up to 7439 m high) separate the Junggar Basin to the
324 north from the Tarim Basin to the south, and the Fergana Basin to the west (Figure 10A). The Junggar
325 Basin has a long history of development (Jolivet et al., 2010; 2013; Jolivet, 2015), from the Paleozoic
326 onwards, and experienced significant Cenozoic deformation as a result of tectonic reactivation of the
327 Tian Shan intracontinental range (Figure 10B). Our recent fieldwork has shown that calcite beef
328 (several cm thick) and cone-in-cone (Figure 10C) occur frequently within mid-Jurassic strata (mainly

329 the Xishanyao and Totounhe Formations), which crop out in the Junggar Basin on its southern margin
330 (Wusu and Totoun localities) or eastern edge (Kalameili region), along a series of thrust faults and
331 folds, related to the development of the Tian Shan and Altai ranges, respectively. Inside the Tian Shan
332 range itself, cone-in-cone structures occur at Nileke (Figure 10D), at the eastern tip of the intra-
333 mountain Yili Basin within the Middle Jurassic Totounhe Formation (Figures 1 and 10). This area has
334 been subject to large-scale thrusting, during Neogene growth of the northern Tian Shan subrange.
335 Finally, to the west in the intramountain Issik-Kul Basin (Kyrgyzstan), bedding-parallel beef with
336 vertical fibers (Figure 10E, F) occur in Jurassic strata along the southern edge of the basin, which has
337 been subject to Cenozoic compressional deformation in the Terzkey range (Figures 1 and 10). The
338 proximity between our beef occurrences and major thrust faults suggests that beef and the Cenozoic
339 reactivation of the basin are synchronous.

340 At all of these localities, the beef or cone-in-cone occur within organic-rich fine-grained alluvial
341 plain deposits (Heilbronn, 2014). In the Junggar and Yili basins, they are also close to coal layers,
342 which are several metres thick. At some localities, especially in the Yili and Issik-Kul basins, the
343 calcite beef is close to iron-rich sandy layers of probable diagenetic origin. At Issik-Kul, strong
344 uranium enrichment of the Jurassic series (Kaji Sai mine) containing the beef again indicates post-
345 sedimentary fluid circulation. In the Junggar Basin, the main source rocks for oil are the upper
346 Permian, Upper Triassic and Middle Jurassic detrital series (Jiao et al., 2007). The occurrence of
347 calcite beef within the Middle Jurassic series and the systematic association between beef and organic-
348 rich siltstone or coal layers suggests a link between hydrocarbon source rocks and calcite beef.

349 In the southern Junggar Basin (locality 8, Figure 1), Jiao et al. (2007) (Fig. 2) described and
350 illustrated thin bedding-parallel veins of calcite within the upper Permian Lucaogou Formation near
351 Urumqi. These authors did not refer to fibrous calcite (beef) or cone-in-cone, but they showed many
352 examples of solid hydrocarbons within cavities, the Lucaogou Formation being a mature petroleum
353 source rock.

354 355 4.4. Appalachian Mountains, United States (locality 2, Fig. 1). 356

357 In the eastern US (Figure. 11A), the Appalachian Mountains trend northeast-southwest and
358 consist mainly of Paleozoic strata, folds and thrusts (Gilman & Metzger, 1967; Evans, 1995; Tobin et
359 al., 1996). At the southwestern end of the mountains, a major unconformity underlies Cretaceous
360 strata, which form a broad anticline (Figure 11A). This provides good evidence for Late Cretaceous or
361 Cenozoic reactivation of the mountain belt. Indeed, even today, the belt is subject to earthquakes,
362 resulting from compressive stress (Heidbach et al., 2009), which appears to derive from ridge-push of
363 the Atlantic spreading center. Veins of calcite beef and bitumen (e.g. Figure 11B) occur within the
364 Devonian Marcellus Shale (Gale et al., 2014; Aydin & Engelder, 2014). Some of the veins are
365 undulating and have additional lenses within synclines (Gale et al., 2014, their fig. 9E). Even today,

366 the Marcellus Shale is a source rock for oil and locally reaches overpressure (Aydin & Engelder,
367 2014), possibly as a result of long-term and recent burial. Furthermore, the layers of Marcellus Shale
368 have acted as detachments for thrust faults in the Appalachians (Aydin & Engelder, 2014). Thus, the
369 Appalachians, like other areas, provide evidence for synchronicity of (1) compressional deformation,
370 (2) generation of organic-rich fluids and (3) formation of calcite beef. A possible problem in the
371 Appalachians is to date these features, which may have started long ago, but still be occurring today.

372

373

374 **5. Discussion**

375

376 Because beef veins seem to be proxies for natural hydraulic fracturing in rocks, especially within
377 source rocks for petroleum, the studies of such fractures are key to the understanding of such
378 geological processes and for the migration and interactions between fluids and rocks. Their formation
379 depends on 2 main phases: (1) the generation of the fracture and (2) the filling of the fracture.

380 For the initiation of the natural hydraulic fractures, and thus the initiation of beef veins, the theory
381 and the experiments of fracturing demonstrate that horizontal (or bedding-parallel) fractures can be
382 generated, due to a distributed fluid overpressure (Cobbold & Rodrigues, 2007; Mourgues et al. 2011;
383 our review; Zanella et al. 2014a). Nevertheless, previous reviews (Cobbold et al. 2003; Gale et al.
384 2014) and more recent and local studies (e.g. Rodrigues et al. 2007; Zanella et al. 2014a, 2014b,
385 2015a, 2015b; Weng et al. 2017; Ukar et al. 2017; Ukar et al. 2018) have shown that the natural
386 hydraulic fracturing often occurred within sedimentary basins which experienced a compressive
387 tectonic history. Moreover, according to several previous studies, the timing of development of beef
388 veins was synchronous with a compressive period in the basin. This is, in particular, well-illustrated
389 for the Neuquén Basin (Rodrigues et al. 2009; Zanella et al. 2015a; Ukar et al. 2017; Ukar et al. 2018),
390 the Wessex Basin (Zanella et al. 2015b), the Bristol Chanel (Weng et al. 2017) and the Magallanes
391 Basin (Zanella et al., 2014). In our study, we demonstrate that this observation is also true for the
392 development of beef veins in the Paris Basin (beef veins dated at 155 Ma), in the northern Pyrenees, in
393 the Uinta Basin, in the Tian Shan Mountains and in the Appalachian Mountains. In view of all of these
394 observations and conclusions, we ask some questions: even if in theory the compressive tectonic stress
395 is not necessary to develop bedding-parallel natural hydraulic fractures, is, in nature, this stress crucial
396 for the development of such fractures? Is the fluid overpressure, generated by hydrocarbons, enough to
397 induce hydraulic fracturing of shales?

398 We thus propose that compressional tectonic stress is one of the key parameters in the
399 development of bedding-parallel veins in shales. This could have major consequences for the
400 understanding of fluid migration in sedimentary rocks, because of the historical complexity of such
401 geological processes. Concerning the generation of hydrocarbons, even if tectonic activity has a big
402 role, the maturation of organic matter, which leads to the development of distributed fluid

403 overpressures and then to natural hydraulic fracturing, is still the main parameter. Indeed, as already
404 demonstrated, during the maturation of the source rock a part of the solid framework (the organic
405 matter) will be transform into fluid (hydrocarbons), implying a collapse and a load transfer responsible
406 of the increasing of the pore fluid pressure (Zanella et al. 2014a). These fractures are always within or
407 near source rocks for petroleum (Cobbold et al. 2013; Gale et al. 2014). All of our examples respect
408 the previous observations. So, as already suggested by previous authors (Ukar et al. 2017, 2018;
409 Zanella et al. 2014b; Zanella et al. 2015a; Zanella et al. 2015b), the link between the presence of beef
410 veins and organic matter is strong. Moreover, the degree of maturity of the source rock is a key
411 parameter for the development of beef veins and other tectonic structures, such as detachments, as
412 demonstrated in the Magellan Basin (Zanella et al. 2014b). In this basin, Zanella et al. (2014b) also
413 demonstrated that there is a link between beef vein composition and the degree of maturity of the
414 source rock. Thus, we infer that this natural fluid generation process is the main driver for inducing
415 fluid overpressure in mature shales, but needs to be assisted by another force, such as the compressive
416 tectonic stress, to be able to induce natural fracturing of the host rocks.

417 Concerning the filling of the fracture and thus the cementation and growth of the bedding-parallel
418 fractures, other mechanisms have to be involved to precipitate minerals. Indeed, the opening of the
419 fractures is in mode 1 and is facilitated by a horizontal compressive stress. Nevertheless, the force of
420 crystallization also participates to pushing outward the vein walls. Currently, which of these two
421 processes plays the dominant role is not yet known.

422

423

424 **6. Conclusions**

425

426 Beef veins (BPV) are common in or near source rocks for petroleum. The study of such geological
427 evidences can help to understand the mechanisms involved in their formation: (1) the generation of the
428 fracture and (2) the opening of the fracture, as well as the migration of fluids in sedimentary basins.
429 Studies of beef vein occurrences around the world have led us to conclude that it is especially common
430 within foreland basins. Here we have reviewed examples (or described new ones) from the Wessex
431 Basin (UK), the Neuquén Basin (Argentina), the Cordillera Oriental (Colombia), the Uinta Basin
432 (USA), the Paris Basin (France), the northern Pyrenees (France), the Tian Shan Mountains (central
433 Asia) and the Appalachian Mountains (USA). However, we have discovered similar beef within other
434 localities of foreland basins (some of which are visible in Fig. 1).

435 In this review, we demonstrate that the development of beef veins occurs worldwide within or
436 near source rocks for petroleum and during a period of hydrocarbon generation. It is now becoming
437 clearer that the maturation of the organic matter can lead to fluid overpressures. Beef veins (and more
438 generally the natural hydraulic fractures) can therefore be used as proxy to determine very quickly if a

439 source rock was or has been mature. On a global scale, many foreland basins contain source rocks,
440 near active or ancient mountain belts, the latter of which may have been reactivated by recent tectonic
441 stress. Many such basins contain enough organic material to have acted as source rocks for petroleum
442 systems, especially where recent burial has generated sufficiently high temperatures. In some
443 examples (such as the Neuquén Basin of Argentina), next to subduction-zone systems, magmatic
444 intrusions or extrusions have added heat and facilitated the maturation of the source rocks, also during
445 compressional tectonic activity.

446 The timing of beef vein generation in foreland basins is always coeval with shortening periods, due
447 to compressive tectonic stress. Thus, even if the theory and the experiments of fracturing demonstrate
448 that bedding-parallel fractures can be generated only with a distributed fluid overpressure, the beef
449 veins formation seems to require an external tectonic stress to develop in nature. The filling of the
450 fractures is likely related to force of crystallization, during the compressive period and facilitates the
451 vertical opening of veins.

452
453

454 **Acknowledgements**

455 During the years 2005 to 2012, Ian West of Southampton University introduced us to some of the
456 best beef localities in the Wessex Basin, along the coast of southern England (West, 2015). We thank
457 Tony Boassen (Statoil Research Centre, Trondheim), for help with scanning electron microscopy of
458 calcite beef from the Wessex Basin and Neuquén. We also thank Andres Mora of Ecopetrol for
459 showing Peter Cobbold some beef veins at the eastern edge of the Cordillera Oriental, Colombia (Fig.
460 5). Fieldwork in central Asia was funded by the DARIUS group. Elsewhere, much of the fieldwork
461 and experimental work, as well as PhD studies, were funded by Statoil (Norway). DC acknowledges
462 support from Science Foundation Ireland under Grant Number 15/IACA/3365.

463
464

465 **References**

466

467 Aydin, M.G., Engelder, T., 2014. Revisiting the Hubbert-Rubey pore pressure model for overthrust
468 faulting: Inferences from bedding-parallel detachment surfaces within Middle Devonian gas
469 shale, the Appalachian Basin, USA. *J. Struct. Geol.* 69, 519-537.

470 Barker, S.L.L., Cox, S.F., Eggins, S.M., Gagan, M.K., 2006. Microchemical evidences for episodic
471 growth of antitaxial veins during fracture-controlled fluid flow. *Earth and Planetary Science*
472 *Letters* 250, 331-344.

473 Biteau, J.-J., Canérot, J., 2007. La Chaîne des Pyrénées et ses avant-pays d'Aquitaine et de l'Ebre:
474 systèmes pétroliers et gisements d'hydrocarbures. *Géologues* 155, 29-41.

475 Bons, P., 2001. Development of crystal morphology during uniaxial growth in a progressively
476 widening vein: I. The numerical model. *Journal of Structural Geology*, 23(6-7): 865-872.

477 Bons, P.D., Elburg, M.A. and Gomez-Rivas, E., 2012. A review of the formation of tectonic veins and
478 their microstructures. *Journal of Structural Geology*, 43: 33-62.

479 Bons, P.D., Jessell, M.W., 1997. Experimental simulation of the formation of fibrous veins by localised
480 dissolution-precipitation creep. *Mineralogical Magazine* 61, 53-63.

481 Bradbury, K.K., Davis, C.R., Shervais, J.W., Janecke, S.U., Evans, J.P., 2015. Composition, alteration,
482 and texture of fault-related rocks from Safod core and surface outcrop analogs: evidence for
483 deformation processes and fluid-rock interactions. *Pure and Applied Geophysics* 172, 1053–1078.

484 Buckland, W., De la Beche, H.T., 1835. On the geology of the neighbourhood of Weymouth and the
485 adjacent parts of the coast of Dorset. *Trans. Geol. Soc. Lond.*, s2 4, 1-46.

486 Chatellier, J.-Y., 2013. How to maximize the use of TMAX, compositional ratios and stable carbon
487 isotopes to accurately infer the maturity of a shale. *Tight Oil Canada*, 2013.

488 Choukroune, P., 1969. Sur la presence, le style et l'âge des tectoniques superposées dans le Crétacé
489 nord-pyrénéen de la région de Lourdes (Hautes-Pyrénées). *Bulletin du Bureau de Recherches*
490 *Géologiques et Minières Section I, No. 2*, 11-20.

491 Cobbold, P.R., 2013. Geological evidence for fluid overpressure in mature source rocks within
492 foreland basins of the Americas. *American Association of Petroleum Geologists, International*
493 *Conference and Exhibition, Cartagena, Colombia, 8-11 September. Search and Discovery Article*
494 *#30291*.

495 Cobbold, P.R., Castro, L., 1999. Fluid pressure and effective stress in sandbox models.
496 *Tectonophysics* 301, 1-19.

497 Cobbold, P.R., Durand, S., Mourgues, R., 2001. Sandbox modelling of thrust wedges with fluid-
498 assisted detachments. *Tectonophysics* 334, 245-258.

499 Cobbold, P.R., Rodrigues, N., 2007. Seepage forces, important factors in the formation of horizontal
500 hydraulic fractures and bedding-parallel fibrous veins (“beef” and “cone-in-cone”). *Geofluids* 7,
501 313-332.

502 Cobbold, P.R., Zanella, A., Ruffet, G., Rodrigues, N., Loseth, H., 2013. Bedding-parallel fibrous veins
503 (beef and cone-in-cone): Worldwide occurrence and possible significance in terms of fluid
504 overpressure, hydrocarbon generation and mineralization. *Mar. Petrol. Geol.* 43, 1-20.

505 Cobbold, P., Zanella, A., Fourdan, B., Néraudeau, D., Gouttefangeas, F., 2015. Natural hydraulic
506 fractures in the Eastern Paris Basin. *Bull. Inf. Géol. Bassin Paris* 52 (2), 23-30.

507 David, L., 1952. Présence de la structure “beef” et “cone-in-cone” dans le Crétacé de l’Est-
508 Constantinois (Algérie). *Comptes Rendus Sommaires de la Société Géologique de France* 3, 51-
509 52.

510 Denaeyer, M.-E., 1943. Les cone-in-cone de la France métropolitaine et d'outre-mer. Bull. Soc. Fr.
511 Minéral. 66 (1-6), 173-221.

512 Denaeyer, M.-E., 1947. Les gisements de cone-in-cone de France et de Grande-Bretagne. Première
513 Partie. Bulletin de la Société Belge de Géologie, Paléontol. Hydrol. 56, 21-46.

514 Dubiel, R.F., 2003. Geology, depositional models, and oil and gas assessment of the Green River total
515 petroleum system, Uinta-Piceance Province, Eastern Utah and Western Colorado. In: Petroleum
516 systems and geologic assessment of oil and gas in the Uinta-Piceance Province, Western
517 Colorado. U.S. Geological Survey, Digital Data Series DDS-69-B, 1-41.

518 Evans, M.A., 1995. Fluid inclusions in veins from the Middle Devonian shales: A record of
519 deformation conditions and fluid evolution in the Appalachian Plateau. Geol. Soc. Am. Bull. 107
520 (3), 327-339.

521 Fischer, M.P., Higuera-Diaz, I.C., Evans, M.A., Perry, E.C., Leticariu, L., 2009. Fracture-controlled
522 paleohydrology in a map-scale detachment fold: Insights from the analysis of fluid inclusions in
523 calcite and quartz veins. J. Struct. Geol. 31, 1490-1510.

524 Fitz-Diaz, E., Hudleston, P., Siebenaller, L., Kirschner, D., Camprubi, A., Tolson, G., Puig, T.P.,
525 2011. Insights into fluid flow and water-rock interaction during deformation of carbonate
526 sequences in the Mexican fold-thrust belt. J. Struct. Geol. 33, 1237-1253.

527 Gale, J.F.W., Laubach, S.E., Olson, J.E., Eichhubl, P., Fall, A., 2014. Natural fractures in shale: a
528 review and new observations. Am. Assoc. Petrol. Geol. Bull. 98 (11), 2165-2216.

529 Gely, J-P., Hanot, F., 2014. Le bassin parisien : un nouveau regard sur la géologie. In: Bulletin
530 d'information des géologues du bassin de Paris, 9, 229 pp.

531 Gilman, R.A., Metzger, W.J., 1967. Cone-in-cone concretions from western New York. J. Sed. Petrol.
532 37, 87-95.

533 Gressier, J.B., Mourgues, R., Bodet, L., Matthieu, J.Y., Galland, O., Cobbold, P.R., 2010. Control of
534 pore fluid pressure on depth of emplacement of magmatic sills: An experimental approach.
535 Tectonophysics 489, 1-13.

536 Guillocheau, F., Robin, C., Allemand, P., Bourquin, S., Brault, N., Dromart, G., Friedenber, R.,
537 Garcia, J.-P., Gaullier, J.-M., Gaumet, F., Grosdoy, B., Hanot, F., Le Strait, P., Mettraux, M.,
538 Nalpas, T., Prijac, C., Rigollet, C., Serrano, O., Grandjean, G., 2000. Meso-Cenozoic geodynamic
539 evolution of the Paris Basin: 3D stratigraphic constraints. Geodinamica Acta 13, 189-246.

540 Heidbach, O., Tingay, M., Bartyh, A., Reinecker, J., Kurfeth, B., Müller, B., 2009. World stress map,
541 2nd Edition. GFZ German Research Centre for Geosciences.

542 Heilbronn, G., 2014. Evolution paléogéographique et paléotopographique du Tian Shan Chinois au
543 Mésozoïque. PhD thesis, Univ. Rennes, 267 pp.

544 Hilgers, C., Koehn, D., Bons, P.D. and Urai, J.L., 2001. Development of crystal morphology during
545 unitaxial growth in a progressively widening vein: II. Numerical simulations of the evolution of
546 antitaxial fibrous veins. Journal of Structural Geology, 23(6-7): 873-885.

547 Hillier, R.D., Cosgrove, J.W., 2002. Core and seismic observations of overpressure-related
548 deformation within Eocene sediments of the Outer Moray Firth, UKCS. *Petroleum Geoscience* 8,
549 141-149.

550 Jiao, Y.Q., Wu, L.Q., He, M.C., Mason, R., Wang, M.F., Xu, Z.C., 2007. Occurrence, thermal
551 evolution and primary migration processes derived from studies of organic matter in the
552 Lucaogou source rock at the southern margin of the Junggar Basin, NW China. *Science in China,*
553 *Series D - Earth Sciences* 50, 114-123.

554 Jolivet, M., Dominguez, S., Charreau, J., Chen, Y., Li, Y., Wang, Q., 2010. Mesozoic and Cenozoic
555 tectonic history of the central Chinese Tian Shan: Reactivated tectonic structures and active
556 deformation. *Tectonics* 29, 1-30.

557 Jolivet, M., Heilbronn, G., Robin, C., Barrier, L., Bourquin, S., Guo, Zh., Jia, Y., Guerit, L., Yang, W.,
558 Fu, B., 2013. Reconstructing the Late Palaeozoic – Mesozoic topographic evolution of the
559 Chinese Tian Shan: available data and remaining uncertainties. *Advances in Geosciences* 37, 7-
560 18.

561 Jolivet, M., 2015. Mesozoic tectonic and topographic evolution of Central Asia and Tibet: a
562 preliminary synthesis. *In: Brunet, M.-F., McCann, T. & Sobel, E.R. (eds) Geological evolution of*
563 *Central Asian Basins and the Western Tien Shan Range. Geol. Soc. London Sp. Publ., 427,*
564 <http://doi.org/10.1144/SP427.2>

565 Kemp, J., 2014. The Big One: Russia's Bazhenov shale.
566 <http://www.reuters.com/article/2014/07/18/us-russia-shale-kemp-idU>.

567 Kershaw, S., Guo, L. 2016. Beef and cone-in-cone calcite fibrous cements associated with the end-
568 Permian and end-Triassic mass extinctions: Reassessment of processes of formation. *J.*
569 *Palaeogeog.* 5 (1), 28-42.

570 Keulen, N. T., den Brok, S.W.J., Spiers, C.J., 2001. Force of crystallisation of gypsum during
571 hydration of synthetic anhydrite rock. 13th DRT conference, Deformation Mechanisms,
572 Rheology, and Tectonics, Noordwijkerhout, The Netherlands.

573 Kowal-Linka, M., 2010. Origin of cone-in-cone calcite veins during calcitization of dolomites and
574 their subsequent diagenesis: A case study from the Gogolin Formation (Middle Triassic), SW
575 Poland. *Sed. Geol.* 224, 54-64.

576 Kozłowski, E.E., Cruz, C.E., Sylwan, C., 1998. Geología estructural de la zona de Chos Malal, Cuenca
577 Neuquina, Argentina. *In: XIII Congreso Geológico Argentino y III Congreso de Exploración de*
578 *Hidrocarburos, Buenos Aires, Actas 1, 15-26.*

579 Labaume, P., Sheppard, S.M.F., Moretti, I., 2001. Fluid flow in cataclastic thrust fault zones in
580 sandstones, Sub-Andean Zone, southern Bolivia. *Tectonophysics* 340, 141-172.

581 Lamb, S., 2004. Devil in the mountain. A search for the origin of the Andes. Princeton University
582 Press 335 pp.

583 Lang, W.D., Spath, L.F., Richardson, W.A., 1923. Shales-With-'Beef', a sequence in the Lower Lias of
584 the Dorset Coast. Q. J. Geol. Soc. Lond. 79, 47-99.

585 Le Breton, E., Cobbold, P.R., Zanella, A., 2013. Cenozoic reactivation of the Great Glen Fault,
586 Scotland: additional evidence and possible causes. J. Geol. Soc. Lond. 170, 403-415, doi:
587 10.1144/jgs2012-067.

588 Lee, G.W., 1920. The Mesozoic rocks of Applecross, Raasay and North-East Skye. H.M. Geological
589 Survey, Scotland, 93 pp.

590 Lemrabortt, A., Cobbold, P.R., 2010. Physical modeling of fluid overpressure and compaction during
591 hydrocarbon generation in source rock of low permeability. Search and Discovery, Article
592 #40518.

593 Leythaeuser, D., Littke, R., Radke, M., Schaefer, R.G., 1988. Geochemical effects of petroleum
594 migration and expulsion from Toarcian source rocks in the Hils Syncline area, NW-Germany. In:
595 Mattavelli, L. & Novelli, L. (Eds.), Advances in Organic Geochemistry 1987. Organic
596 Geochemistry 13, 489-502.

597 Lilloe-Olsen, T., Bang, N.A., 2012. DNO and Tawke in Kurdistan: How an Iraq oil giant has emerged.
598 Oil & Gas Journal 1-19. [http://www.ogi.com/articles/print/vol-110/issue-2/exploration-](http://www.ogi.com/articles/print/vol-110/issue-2/exploration-developmet/dno-and-tawke-in...)
599 [developmet/dno-and-tawke-in...](http://www.ogi.com/articles/print/vol-110/issue-2/exploration-developmet/dno-and-tawke-in...)

600 Macsotay, O., Erlich, R.N., Peraza, T., 2003. Sedimentary structures of the La Luna, Navay and
601 Querecual Formations, Upper Cretaceous of Venezuela. Palaios 18, 334-348.

602 Mahboubi, A., Moussavi-Harami, R., Collins, R.B., Muhling, J.R., 2010. Petrography and
603 geochemical signatures in cracks filling calcite sequences in septarian concretions, Sanganeh
604 Formation, Kopet-Dagh Basin, NE Iran. J. Appl. Sci. 10, 526-534.

605 Maillot, H., Bonte, A., 1983. Cone-in-cone texture from Deep Sea Drilling Project Leg 71, Site 511,
606 Falkland Plateau, South Atlantic Ocean. Initial Reports of the Deep Sea Drilling Project 71(1),
607 345-349.

608 Mangenot, X., Gasparrini, M., Rouchon, V., Bonifacie, M., 2018. Basin-scale thermal and fluid flow
609 histories revealed by carbonate clumped isotopes ($\Delta 47$)—Middle Jurassic carbonates of the Paris
610 Basin depocentre. *Sedimentology*, 65(1), 123-150.

611 Marques, F.O., Nogueira, F.C.C., Bezerra, F.H.R., Castro, D.L. de, 2014. The Araripe Basin in NE
612 Brazil: An intracontinental graben inverted to a high-standing horst. *Tectonophysics* 630, 251–
613 264.

614 Marshall, J.D., 1982. Isotopic composition of displacive fibrous calcite veins; reversals in pore-water
615 composition trends during burial diagenesis. *J. Sediment. Petrol.* 52, 615-630.

616 Martinius, A.W., Hegner, J., Kaas, I., Bejarano, C., Mathieu, X., Mjoes, R., 2012. Sedimentology and
617 depositional model for the Early Miocene Oficina Formation in the Petrocedeno Field (Orinoco
618 heavy-oil belt, Venezuela). *Mar. Petrol. Geol.* 35, 354-380.

619 Means, W. and Li, T., 2001. A laboratory simulation of fibrous veins: some first observations. *Journal*

620 of Structural Geology, 23(6-7): 857-863.

621 Mora, A., Blanco, V., Naranjo, J., Sanchez, N., Ketcham, R.A., Rubiano, J., Stockli, D.F., Quintero, I.,
622 Nemcok, M., Horton, B.K., Davila, H., 2013. On the lag time between internal strain and
623 basement involved thrust induced exhumation: The case of the Colombian Eastern Cordillera. *J.*
624 *Struct. Geol.* 52, 96-118.

625 Mora, A., Casallas, W., Ketcham, R.A., Gomez, D., Parra, M., Namson, J., Stockli, D., Almendral, A.,
626 Robles, W., Ghorbal, B., 2015. Kinematic restoration of contractional basement structures using
627 thermokinematic models. *Am. Assoc. Petrol. Geol. Bull.* 99 (8), 1575–1598.

628 Mourgues, R., Cobbold, P.R., 2003. Some tectonic consequences of fluid overpressures and seepage
629 forces as demonstrated by sandbox modeling. *Tectonophysics* 376, 75-97.

630 Nollet, S., Urai, J.L., Bons, P.D., Hilgers, C., 2005. Numerical simulations of polycrystal growth in
631 veins. *Journal of Structural Geology* 27, 217-230.

632 Nollet, S., Koerner, T., Kramm, U., Hilgers, C., 2009. Precipitation of fracture fillings and cements in
633 the Buntsandstein (NW Germany). *Geofluids* 9, 373-385.

634 Nomura, S.F., Sawakuchi, A.O., Bello, R.M.S., Méndez-Duque, J., Fuzikawa, K., Giannini, P.C.F.,
635 Dantas, M.S.S., 2014. Paleotemperatures and paleofluids recorded in fluid inclusions from calcite
636 veins from the northern flank of the Ponta Grossa dyke swarm: Implications for hydrocarbon
637 generation and migration in the Paraná Basin. *Mar. Petrol. Geol.* 52, 107-124.

638 Parnell, J., Blamey, N.J.F., Costanzo, A., Feely, M., Boyce, A.J., 2014. Preservation of
639 Mesoproterozoic age deep burial fluid signatures, NW Scotland. *Mar. Petrol. Geol.* 55, 275-281.

640 Pearson, P.N., Nicholas, C.J., Singano, J.M., Bown, P.R., Coxall, H.K., van Dongen, B.E., Huber,
641 B.T., Karega, A., Lees, J.A., MacLeod, K., McMillan, I.K., Pancost, R.D., Pearson, M., Msaky,
642 E., 2006. Further Paleogene and Cretaceous sediment cores from the Kilwa area of coastal
643 Tanzania: Tanzania Drilling Project Sites 6–10. *J. Afr. Earth Sci.* 45, 279-317.

644 Richardson, W.A., 1923. Petrology of the Shales-with-“Beef.” *Q. J. Geol. Soc. Lond.* 79, 88-99.

645 Rodrigues, N., Cobbold, P.R., Loseth, H., Ruffet, G., 2009. Widespread bedding-parallel veins of
646 fibrous calcite (“beef”) in a mature source rock (Vaca Muerta Fm, Neuquén Basin, Argentina):
647 evidence for overpressure and horizontal compression. *J. Geol. Soc. Lond.* 166, 695-709, doi
648 10.1144/0016-76492008-111.

649 Rybak-Ostrowska, B., Konon, A., Nejbort, K., Kozłowski, A., 2014. Bedding-parallel calcite veins in
650 the Holy Cross Mountains Fold Belt, central Poland. *Geological Quarterly* 58 (1), 99–116.

651 Silva, A.L. Da, 2003. Estratigrafia física e deformação do sistema lacustre carbonático (Aptiano-
652 Albiano) da Bacia do Araripe em afloramentos selecionados. Dissertação de Mestrado, Univ. Fed.
653 Pernambuco, Pós-graduação em Geociências, 118 pp.

654 Smith, A.P., Fischer, M.P., Evans, M.A., 2014. On the homogeneity of fluids forming bedding-parallel
655 veins. *Geofluids* 14, 45-57.

- 656 Suchy, V., Dobes, P., Filip, J., Stejskal, M., Zeman, A., 2002. Conditions for veining in the Barrandian
657 Basin (Lower Palaeozoic), Czech Republic: evidence from fluid inclusion and apatite fission
658 track analysis. *Tectonophysics* 348, 25-50.
- 659 Tarney, J., Schreiber, B.C., 1976. Cone-in-cone and beef-in-shale textures from DSDP site 330,
660 Falkland Plateau, South Atlantic. In: Barker, P.F., Dalziel, I.W.D. et al. (Eds), *Initial Reports of*
661 *the Deep Sea Drilling Project*. U.S. Government Printing Office, Washington, D.C. 36, 865-870.
- 662 Tobin, K.J., Walker, K.R., Steinhauff, D.M., Mora, C.I., 1996. Fibrous calcite from the Ordovician of
663 Tennessee: preservation of marine oxygen isotopic composition and its implications.
664 *Sedimentology* 43, 235-251.
- 665 Trabucho-Alexandre, J., Dirkx, J., Veld, H., Klaver, G., De Boer, P.L., 2012. Toarcian black shales in
666 the Dutch Central Graben: Record of energetic, variable depositional conditions during an
667 oceanic anoxic event. *J. Sed. Res.* 82, 104-120.
- 668 Ukar, E., Lopez, R.G., Gale, J.F., Laubach, S. E., Manceda, R., 2017. New type of kinematic indicator
669 in bed-parallel veins, Late Jurassic–Early Cretaceous Vaca Muerta Formation, Argentina: EW
670 shortening during Late Cretaceous vein opening. *Journal of Structural Geology*, 104, 31-47.
- 671 Ukar, E., López, R., Hryb, D., Gale, J.F., Manceda, R., Fall, A., Brisson, I., Hernandez-Bilbao, E.,
672 Weger, R., Marchal, D., Zanella, A., Lanusse, I., 2018. Natural fractures in the Vaca Muerta
673 Formation: from core and outcrop analog observations to subsurface models. *AAPG Memoir*,
674 120, (submitted).
- 675 Underhill, J.R., Stoneley, R., 1998. Introduction to the development, evolution and petroleum geology
676 of the Wessex Basin. In: *Geol. Soc., London, Sp. Publ.* 133, 1-18.
- 677 Vera, E.A.R., Folguera, A., Valcarce, G.Z., Bottesi, G., Ramos, V. A., 2014. Structure and
678 development of the Andean system between 36 and 39 S. *Journal of Geodynamics*, 73, 34-52.
- 679 Voisin, L., 1999. Le “beef” de Chaumiau (08). *Bull. d’Inform. Géol. Bassin de Paris* 36 (2), 13-16.
- 680 Volk, H., Horsfield, B., Mann, U., Suchy, V., 2002. Variability of petroleum inclusions in vein, fossil
681 and vug cements - a geochemical study in the Barrandian Basin (Lower Palaeozoic, Czech
682 Republic). *Organic Geochemistry* 33, 1319-1341.
- 683 Watts, N.L., 1978. Displacive calcite: Evidence from recent and ancient calcretes. *Geology* 6, 699-
684 703.
- 685 Weger, R.J., Murray, S.T., McNeill, D.J., Swart, P.K., Eberli, G.P., Rodriguez Blanco, L., Tenaglia,
686 M., Rueda, L., 2018. Paleo thermometry and distribution of calcite beef in the Vaca Muerta
687 Formation, Neuquén Basin, Argentina. *AAPG Bulletin*, (submitted).
- 688 West, I.M., 2015. Geology of the Wessex coast of southern England – the World Heritage Jurassic
689 Coast – and more. Internet page: <http://www.southampton.ac.uk/~imw/index.htm>.
- 690 Woodland, B.G., 1964. The nature and origin of cone-in-cone structure. *Fieldiana: Geology* 13 (4),
691 187-305.
- 692 Zanella, A., Cobbold, P.R., Le Carlier de Veslud, C., 2014a. Physical modelling of chemical

693 compaction, overpressure development, hydraulic fracturing and thrust detachments in organic-
694 rich source rock. *Mar. Petrol. Geol.* 55, 262-274.
695 <http://dx.doi.org/10.1016/j.marpetgeo.2013.12.017>.
696 Zanella, A., Cobbold, P.R., Rojas, L., 2014b. Beef veins and thrust detachments in Early Cretaceous
697 source rocks, foothills of Magallanes-Austral Basin, southern Chile and Argentina: structural
698 evidence for fluid overpressure during hydrocarbon maturation. *Mar. Petrol. Geol.* 55, 250-261.
699 <http://dx.doi.org/10.1016/j.marpetgeo.2013.10.006>.
700 Zanella, A., Cobbold, P.R., Ruffet, G., Leanza, H.A., 2015a. Geological evidence for fluid
701 overpressure, hydraulic fracturing and strong heating during maturation and migration of
702 hydrocarbons in Mesozoic rocks of the northern Neuquén Basin, Mendoza Province, Argentina. *J.*
703 *S. Am. Earth Sci.* 62, 229-242.
704 Zanella, A., Cobbold, P.R., Boassen, T., 2015b. Natural hydraulic fractures in the Wessex Basin, SW
705 England: widespread distribution, composition and history. *Mar. Petrol. Geol.* 68, 438-448.
706 Zhang, B., Yin, C.Y., Gu, Z.D., Zhang, J.J., Yan, S.Y., Wang, Y., 2015. New indicators from bedding-
707 parallel beef veins for the fault valve mechanism. *Science China: Earth Sci.*, doi: 10.1007/s11430-
708 015-5086-6.

709
710

711 **Figure captions**

712

713 **Table 1.** Global distribution of compressional basins, where calcite beef or cone-in-cone occur. For
714 localities (numbers at left), see Figure 1. Not all references are to previous descriptions of calcite beef.
715

716 **Figure 1.** Map showing distribution of calcite beef (bedding-parallel veins), either within Mesozoic or
717 Cenozoic sedimentary rocks (light triangles) or within Paleozoic sedimentary rocks (dark triangles).
718 The numbers next to the triangles refer to the localities in Table 1.

719

720 **Figure 2.** A. Physical model of horizontal hydraulic fracturing with no deformation (after Zanella et
721 al., 2014a); B. Physical model of horizontal hydraulic fracturing with shortening (after Zanella et al.,
722 2014a); C. Cross-section of a 3-D physical model showing the different styles of deformation due to
723 the propagation of a detachment linked to overpressure development (after Zanella et al., 2014a).

724

725 **Figure 3.** A. Geological map and cross-section of the Wessex Basin, southwestern England (after
726 Zanella et al. 2015B, modified from Underhill et al. 1998). B. folded and faulted beef veins, the
727 thickness of which is again variable, especially across the main reverse fault (center). C. Locally
728 folded beef, the thickness of which is variable (thicker in syncline, thinner in anticline). D. Steeply
729 dipping but curved calcite fibers, which comprise a layer of beef. (scales: pen: 14cm; coin diameter:

730 2.4 cm).

731

732 **Figure 4.** A. Calcite beef in the Neuquén Basin, Argentina (white locality 4, Figure 1) (after
733 Rodrigues et al., 2009). The Landsat image (left) shows sub-Andean folds, trending north-northwest.
734 Field observations (bottom right) show that beef is common in the Vaca Muerta Formation at various
735 scales. B. Geological section through the fold and thrust belt of the Neuquén Basin (located with the
736 red line in Figure 4A.) (after Vera et al., 2014).

737

738 **Figure 5.** A. Geological map and cross-section, showing the main structures of the eastern Cordillera
739 (after Mora et al., 2013, 2015). B. Calcite beef (bedding-parallel) veins (white to yellow), which vary
740 in thickness across folds (Cobbold, 2013). C. On the western side of the Cordillera, near Villeta, folds
741 and thrusts verge westward and Cretaceous shales contain layers of calcite beef. D. At the eastern edge
742 of the Cordillera, in the Macanal Formation (Lower Cretaceous) near Villavicencio, some beef
743 contains thin layers of yellow pyrite, which are folded, while calcite has grown epitaxially above and
744 below them, filling in synclines more than anticlines. (scales: coin diameter: 2.2 cm).

745

746 **Figure 6.** A. Geological map of the Paris Basin (after Gely and Hanot, 2014; Mangenot et al. 2018).
747 The basin has an elliptical shape with a long axis trending approximately northeast-southwest. The line
748 of section is indicated in red. B. Gélaucourt, near Nancy, where ditches have exposed Liassic shales of
749 the Schistes Carton Formation (lower Toarcian, Denaeyer, 1943; ca 185 Ma.), which contain abundant
750 veins of fibrous calcite beef (hammer length: 33 cm). C. Calcite beef from the Toarcian at Gélaucourt
751 (coin diameter: 2.3 cm).

752

753 **Figure 7.** A. U-Pb Tera-Wasserburg calcite lower intercept age of 155 ± 19 Ma (Oxfordian) for the
754 formation of the calcite beef (Chew et al., work in progress). B&C. Scanning electron microscopy
755 (SEM) analyses of calcite beef (bedding-parallel veins) from the Liassic “Schistes Carton” near
756 Gélaucourt in the Paris Basin (see Fig. 6). Scanning electron microscopy (SEM) has yielded
757 significant quantities of calcium (B) and carbon (C), which are typical of calcite. However, the amount
758 of carbon is locally greater (pink, top right), due to inclusions of hydrocarbons within the calcite
759 crystals (Cobbold et al., 2015).

760

761 **Figure 8.** Calcite beef near Lourdes, at the northern edge of the Pyrenees (white locality 22, Figure 1).
762 A. Google Earth oblique view of the Pic du Béout hills (1530 m high, near the southeast end of
763 Lourdes city), shows repetitions of white, thick, resistant layers of Aptian-Albian limestones, which
764 dip at about 30° to 40° to the south forming scarps. The white line represents the main thrust fault. B.
765 Road outcrop showing fibrous calcite beef (bedding-parallel veins) in upper Aptian shales (coin
766 diameter: 2.3 cm). C. Scanning electron microscopy and the repartition of the carbon, the calcium and

767 the oxygen in the beef vein.

768

769 **Figure 9.** Calcite beef and bitumen in the Uinta Basin, Utah (white locality 13, Fig. 1). A. A
770 simplified geological section (top, north-northeast to southwest, after Dubiel, 2003) shows the
771 asymmetric structure of the basin. B. Outcrop, discovered in 2009, showing gently dipping beds of the
772 Green River Formation (grey) and numerous veins, either of pure fibrous calcite (orange, left), or of
773 fibrous calcite (coin diameter: 2.4 cm). C. Beef veins with gilsonite (whitish and grey; beneath
774 hammer) (hammer length: 33 cm).

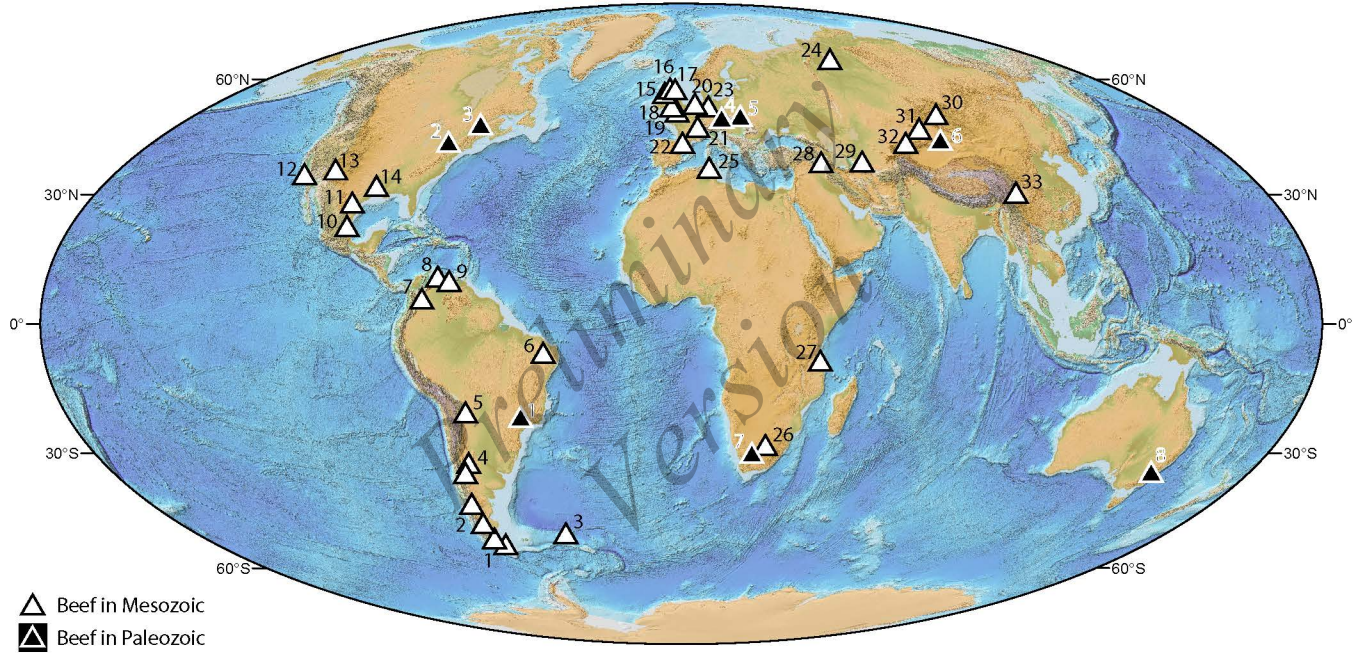
775

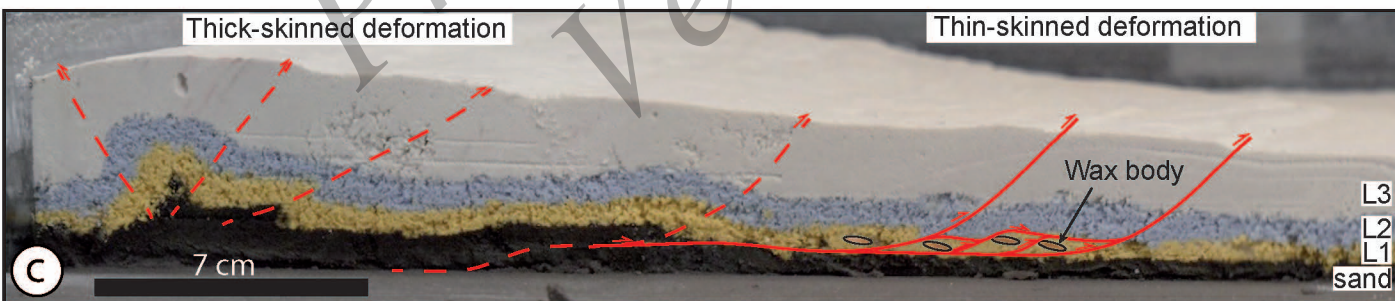
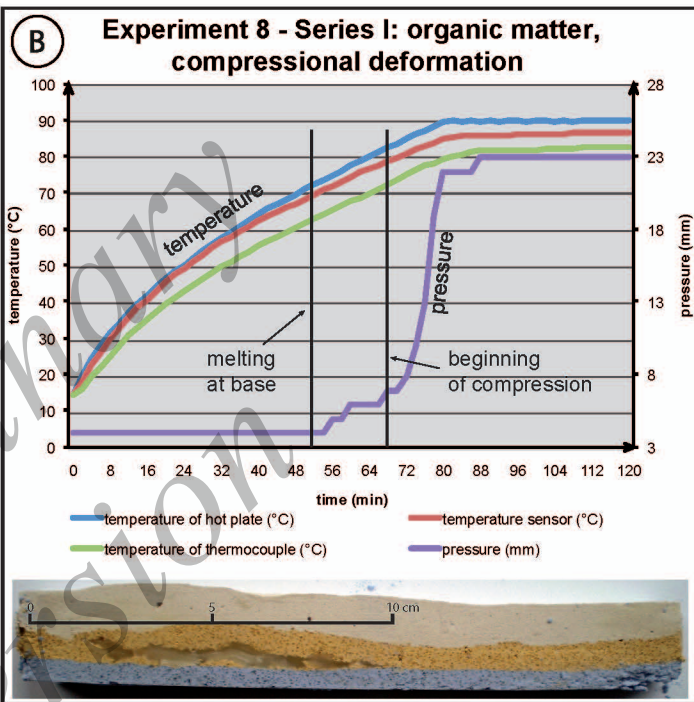
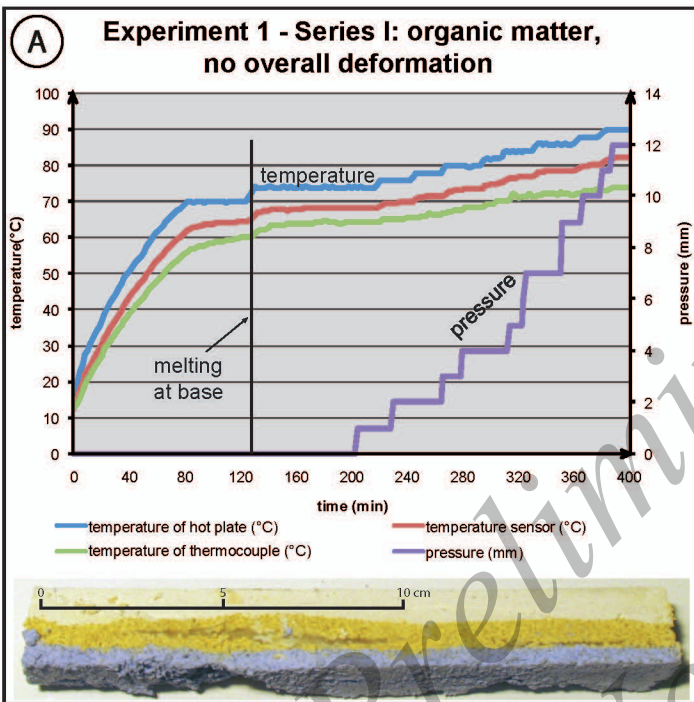
776 **Figure 10.** Calcite beef around the Tian Shan Mountains, central Asia (localities 30 to 32, Fig. 1). A:
777 Topographic and tectonic map of the Tian Shan and Junggar region (modified from Jolivet et al.,
778 2013). B: Geological cross-section (approximately north-south) of the Junggar Basin (red line, A). C:
779 Cone-in-cone structures in the Xishanyao Formation (Middle Jurassic) at Wusu (top) (lens cover
780 diameter: 5.2 cm). D: Cone-in-cone structures in the Totounhe Formation (Middle Jurassic) at Nileke
781 (top). E and F: bedding-parallel calcite beef in Jurassic strata at Kaji Sai (Issik Kul Basin, top) (pen: 14
782 cm).

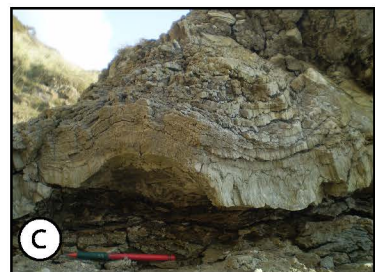
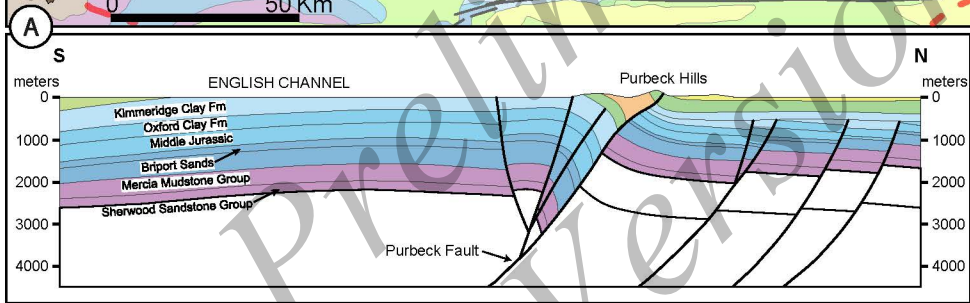
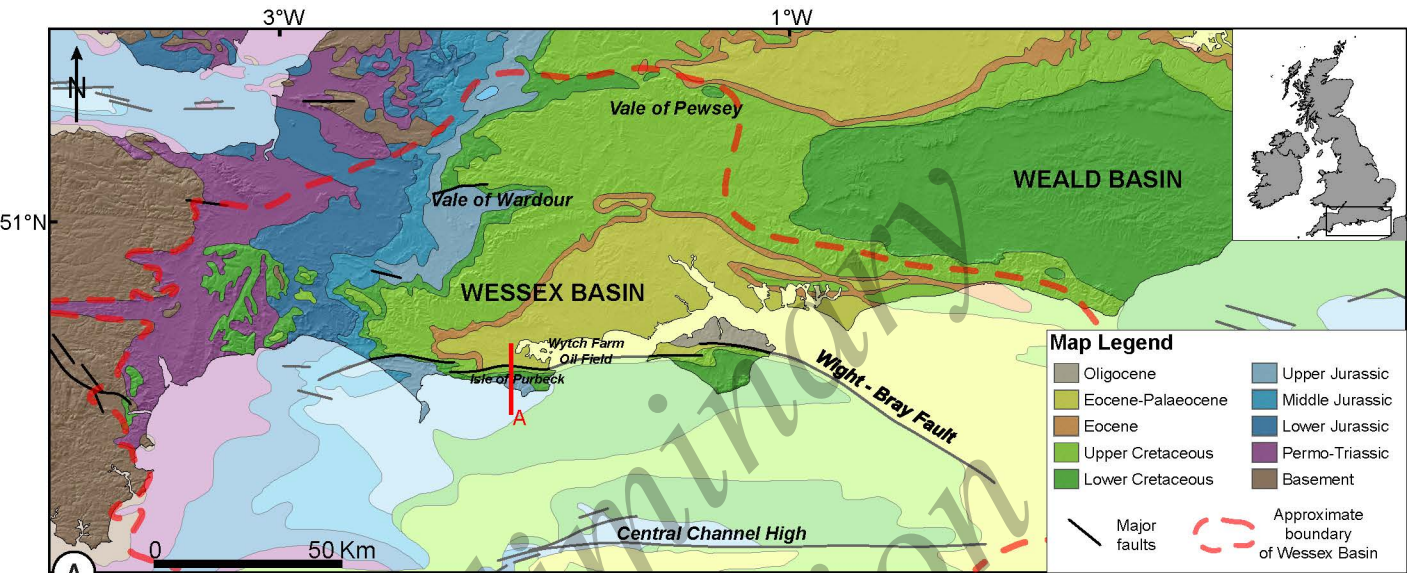
783

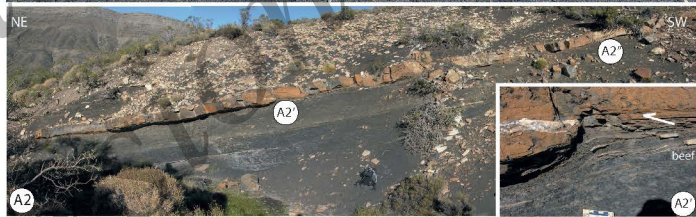
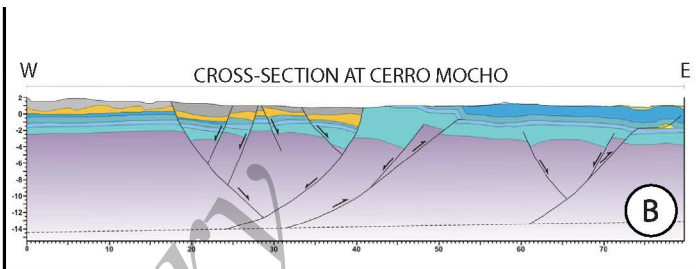
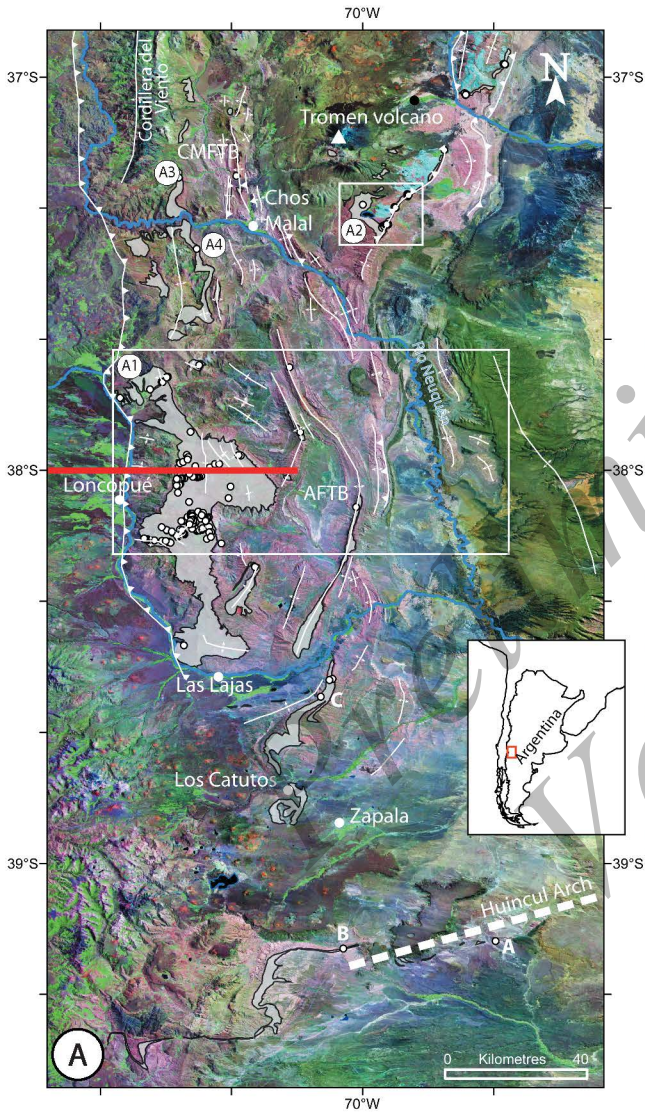
784 **Figure 11.** Calcite beef and bitumen in the Appalachian Mountains, US (locality 2, Figure 1). A.
785 Simplified geological map showing the Paleozoic thrust belt (red), trending northeast-southwest. At its
786 southwestern end, a major unconformity marks the base of Cretaceous strata (green), which
787 nevertheless form a broad anticline, plunging southwest. Red dot refers to Fig. 11B. B. Veins of calcite
788 beef (bedding-parallel veins) and bitumen occurring within the Marcellus Shale (Devonian) along
789 Route 250, Highland County, Virginia (38°19'34.31°N; 79°26'32.29°W, south-southeast of
790 Pittsburgh, Pennsylvania) (coin diameter: 2.4 cm).

791

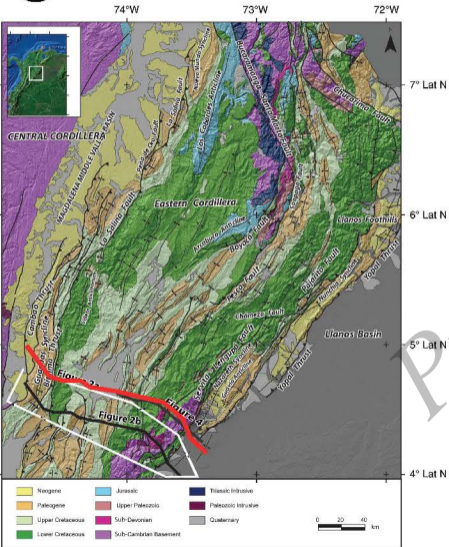




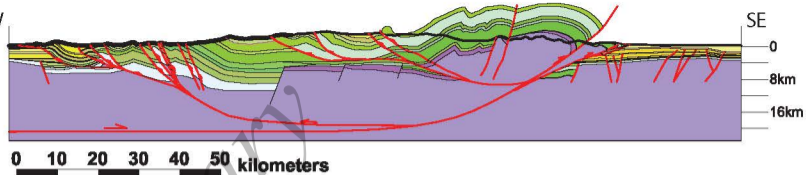


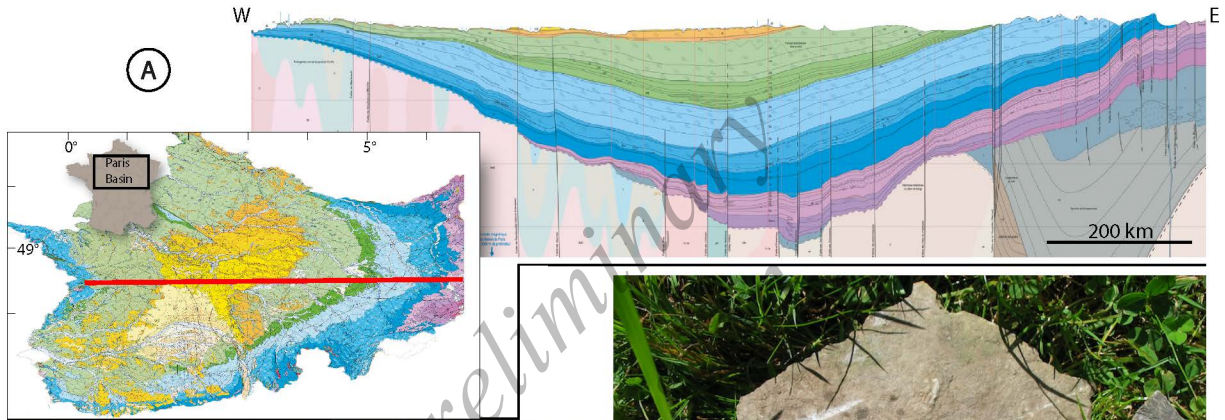


- Areas of outcropping Vaca Muerta Fm
- Studied localities within Vaca Muerta Fm
- River
- Anticline
- Thrust fault
- Strike-slip fault
- AFTB Agrio fold-and-thrust belt
- CMFTB Chos-Malal fold-and-thrust belt

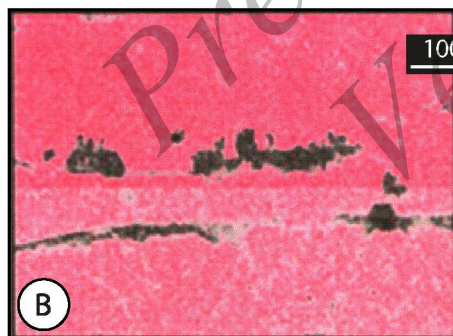
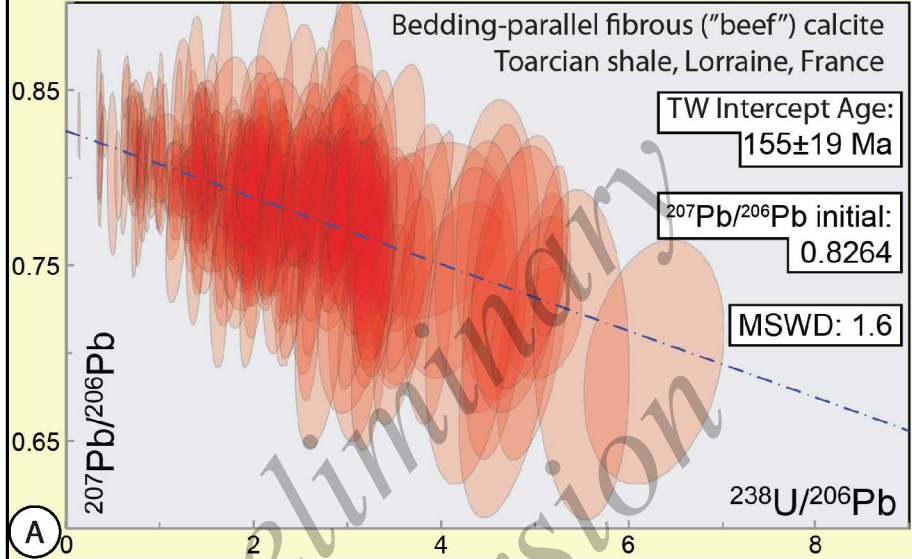
A

NW

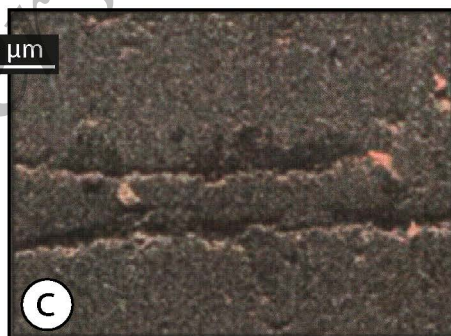




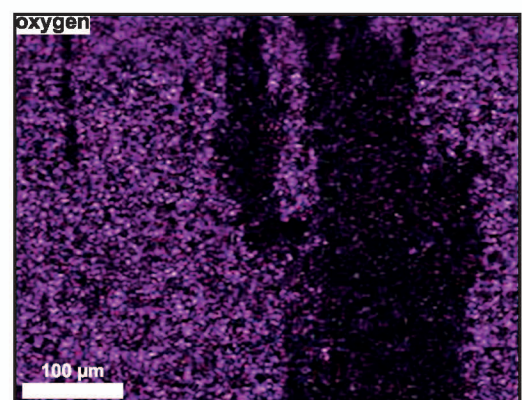
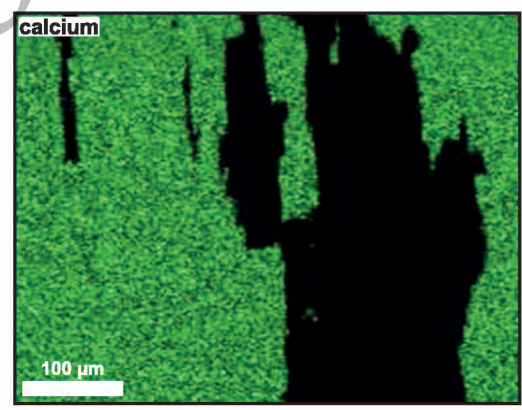
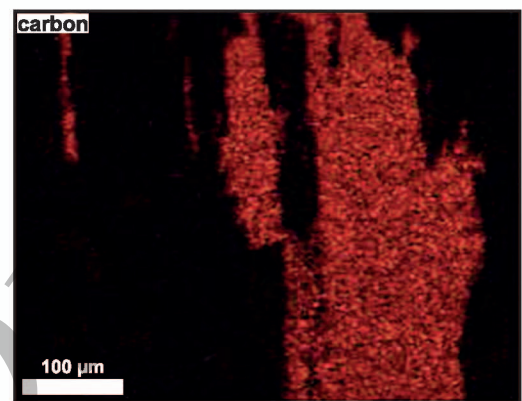
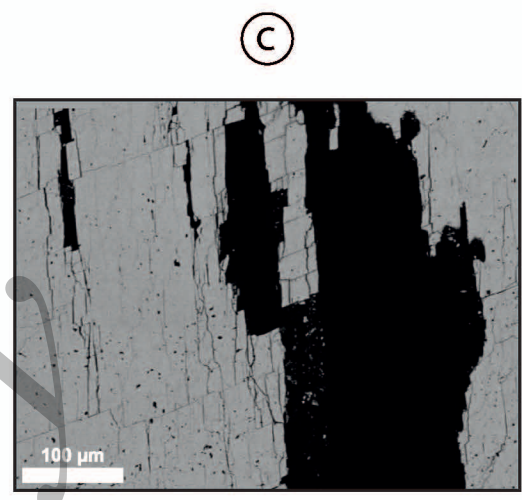
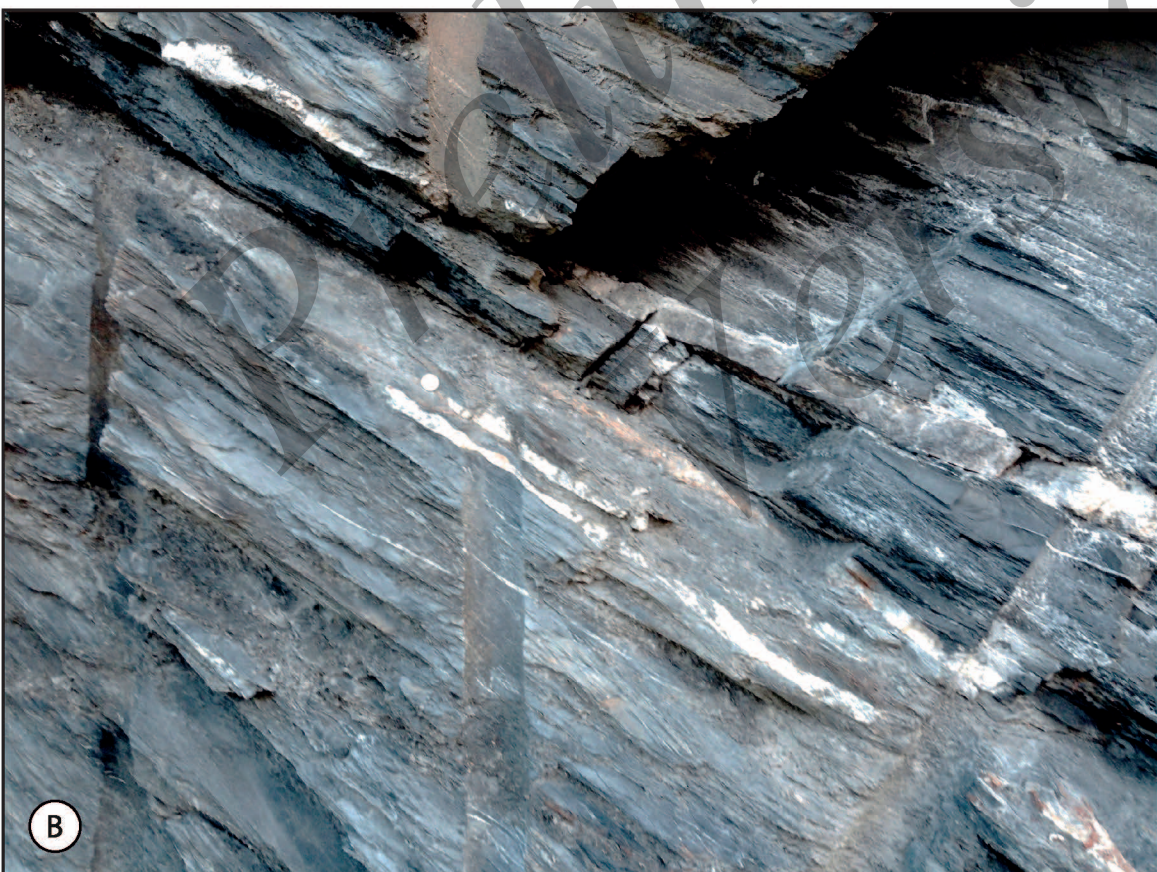
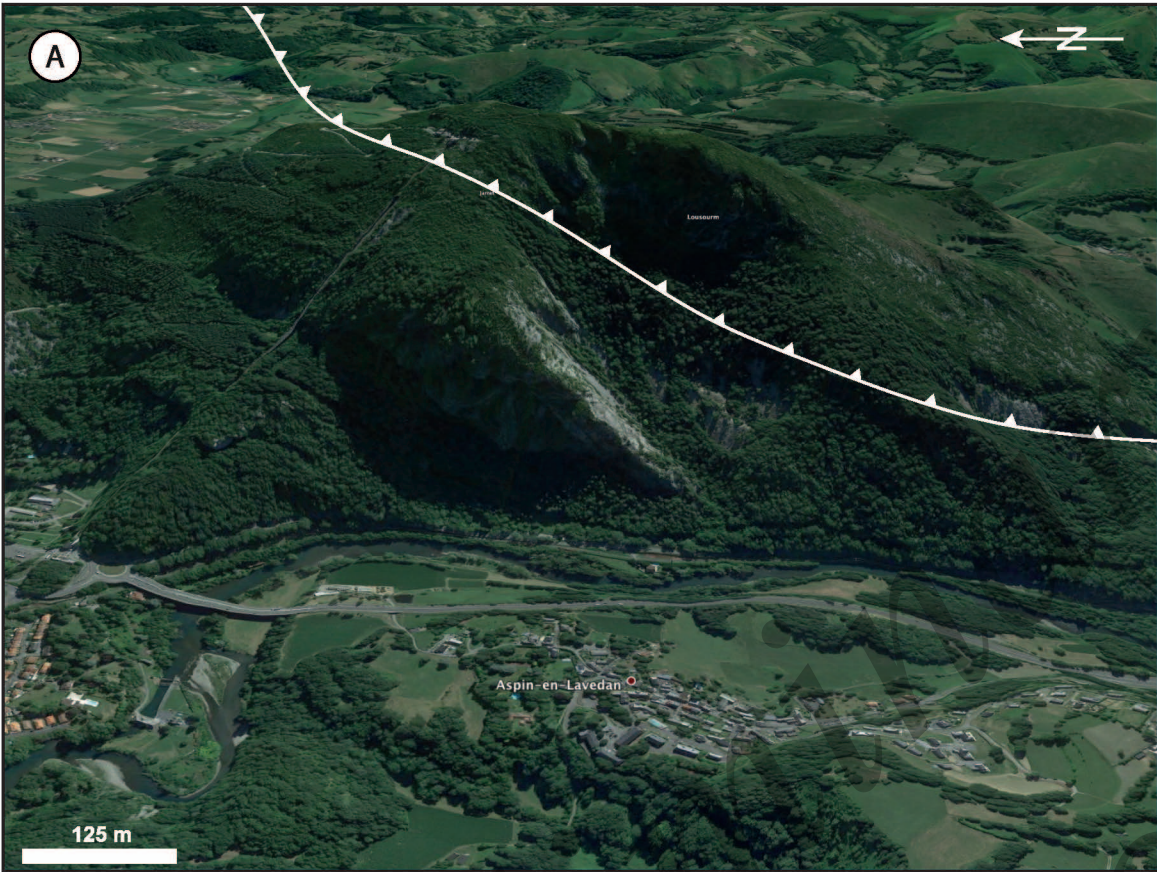
Bedding-parallel fibrous ("beef") calcite
Toarcian shale, Lorraine, France

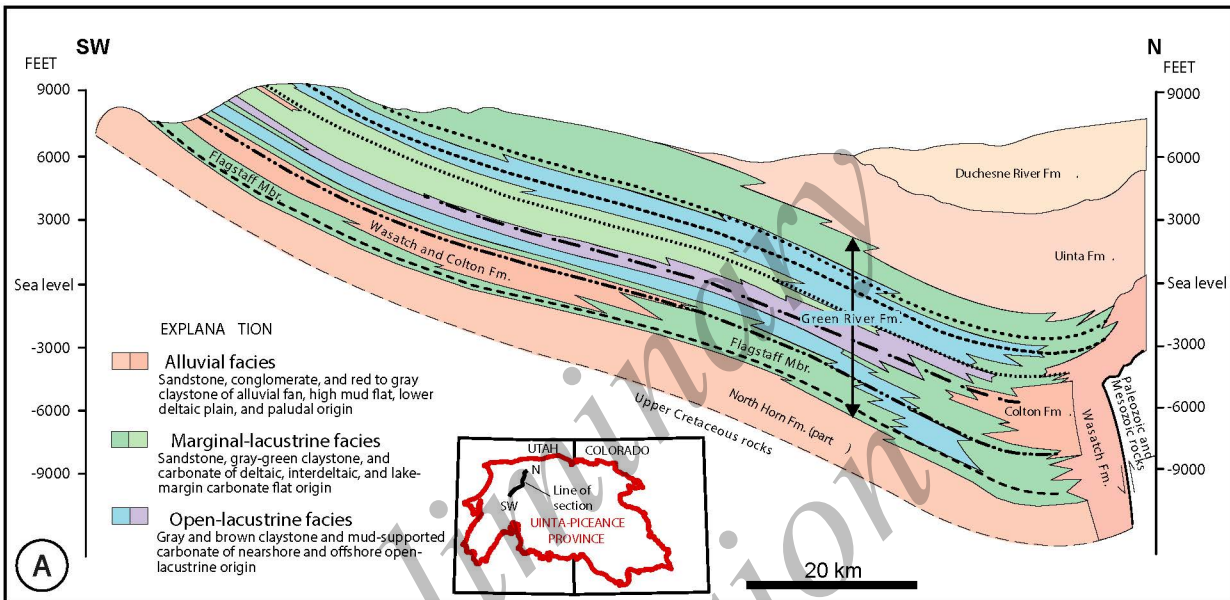


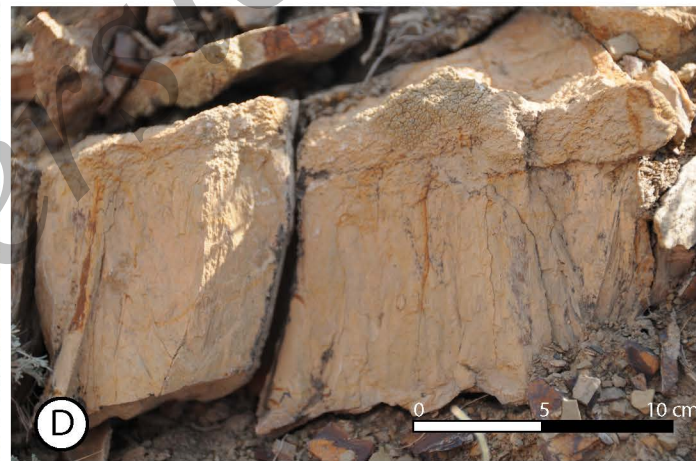
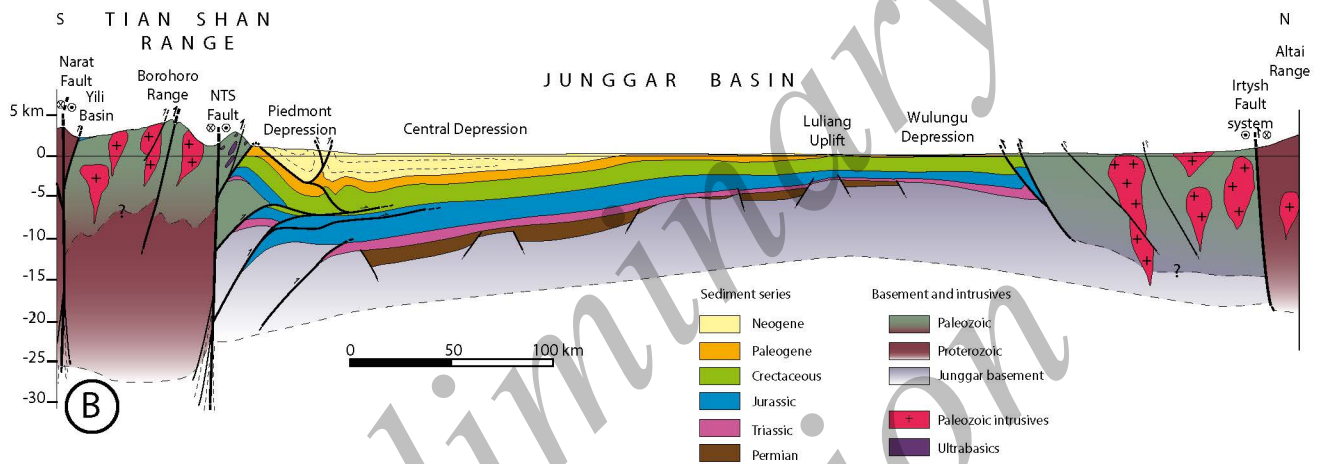
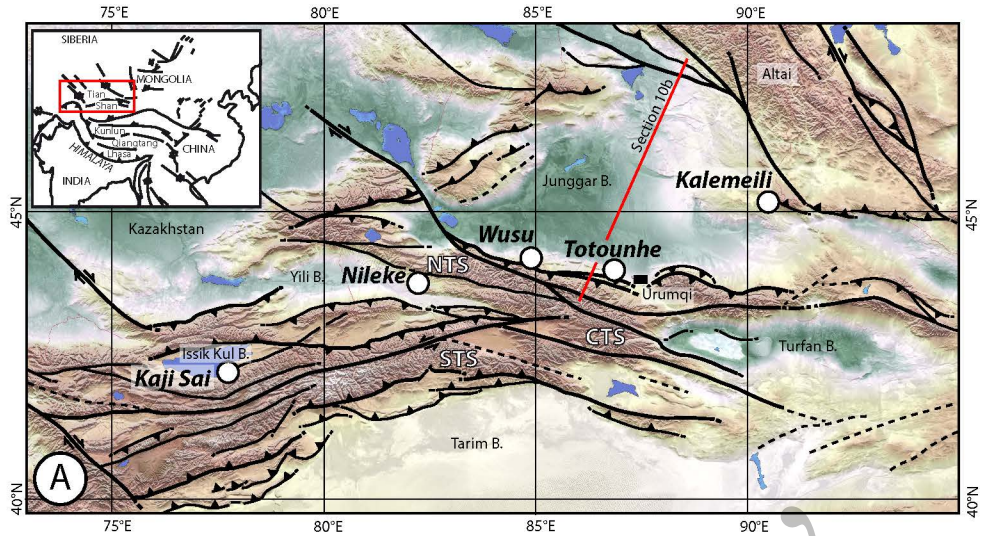
Ca

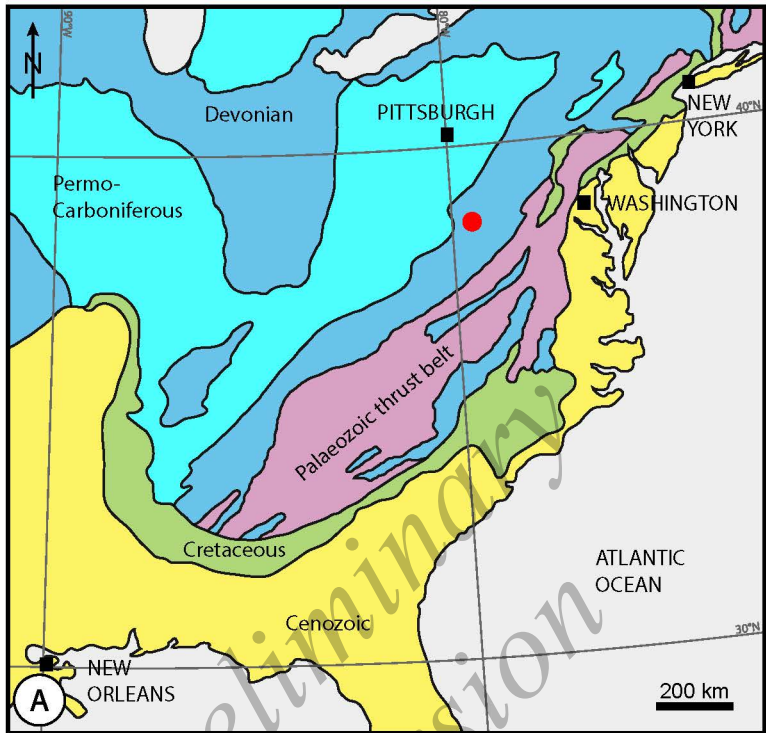


C









No. Location

References

A. Mesozoic or Cenozoic host rocks

- | | | |
|----|---|---|
| 1 | Magallanes Basin (Chile, Tierra del Fuego), Rio Jackson Fm (Early Cretaceous) | Zanella et al., 2014a |
| 2 | Magallanes-Austral Basin (Chubut, Argentina), Rio Mayer Fm (Early Cretaceous) | Zanella et al., 2014a |
| 3 | Falkland Plateau, Maurice Ewing Bank (Late Jurassic to Early Cretaceous) | Tarney & Schreiber, 1976; Maillot & Bonte, 1983 |
| 4 | Neuquén Basin, Argentina, Los Molles, Vaca Muerta, Agrio Fms (Jurassic to Cretaceous) | Fig. 4; Rodrigues et al., 2009; Cobbold et al., 2013; Gale et al., 2014; Ukar et al. 2017; Zanella et al., 2015 |
| 5 | Sub-Andean Zone, southern Bolivia (Tertiary strata) | Labaume et al., 2001; Lamb, 2004 |
| 6 | Araripe Basin, NE Brazil (Early Cretaceous) | Silva, 2003; Marques et al., 2014 |
| 7 | Eastern Cordillera, Colombia, (Early Cretaceous source rock) | Fig. 5; Cobbold et al., 2013; Mora et al., 2013; Mora et al., 2015 |
| 8 | Northern Venezuela, La Luna Fm (Late Cretaceous) | Macsotay et al., 2003 |
| 9 | Northern Venezuela, Oficina Fm (Early Miocene) | Martinius et al., 2012 |
| 10 | Central Mexico Fold-and-Thrust Belt, (Cretaceous) | Fitz-Diaz et al., 2011 |
| 11 | Sierra Madre Oriental, NE Mexico (Jurassic-Cretaceous) | Fischer et al., 2009; Smith et al., 2014 |
| 12 | SW California, USA, Franciscan Complex (Late Jurassic to Cretaceous) | Bradbury et al., 2015 |
| 13 | Uinta Basin, Utah, Green River Fm (Eocene) | Fig. 9; Woodland, 1964; Dubiel, 2003 |
| 14 | Texas, Haynesville Shale (Jurassic) | Gale et al., 2014 |
| 15 | Outer Hebrides (Eigg, Raasay, Skye), Scotland, UK (Jurassic) | Lee, 1920; Marshall, 1982; Parnell et al., 2014 |
| 16 | Eathie, Great Glen, NE Scotland (Jurassic) | Le Breton et al., 2013 |
| 17 | Alba Field, Outer Moray Firth, United Kingdom (Eocene) | Hillier & Cosgrove, 2002 |
| 18 | Lavernock Point, South Wales (Triassic) | Kershaw & Guo, 2016 |
| 19 | Wessex Basin, UK (Liassic to Mid-Cretaceous) | Fig. 3; Buckland & De la Beche, 1835; Richardson, 1923; Marshall, 1982; Underhill & Stoneley, 1998; Cobbold & Rodrigues, 2007; Zanella et al., 2015b; Kershaw & Guo, 2016 |
| 20 | Dutch Central Graben (Toarcian) | Trabucho-Alexandre et al., 2012 |
| 21 | Eastern and Northern Paris Basin, France (Triassic, Liassic) | Figs. 6 & 7; Denaeey, 1943, 1947; Voisin, 1999; Cobbold et al., 2015 |
| 22 | Lourdes, North-Central Pyrenees, France (Aptian-Albian) | Fig. 8; Choukroune, 1969; Biteau & Canérot, 2007 |
| 23 | Hils Syncline, NW Germany (Toarcian) | Leythaeuser et al., 1988 |
| 24 | West Siberia Basin, Russia, Bazhenov Shale (Tithonian-Berriasian) | Kemp, 2014; Fjellanger et al., 2015 |
| 25 | Algeria-Tunisia (Cretaceous) | David, 1952 |
| 26 | Kalahari Desert, South Africa and Botswana (Quaternary) | Watts, 1978 |
| 27 | Kilwa, coastal Tanzania (Cretaceous, Paleogene) | Pearson et al., 2006 |
| 28 | Tawke Field, Kurdistan, NW Iraq, Sargelu Fm (Jurassic) | Lilloe-Olsen & Bang, 2012 |
| 29 | Kopet-Dagh Basin, NE Iran, Sanganeh Fm (Late Cretaceous) | Mahboubi et al., 2010 |
| 30 | Junggar Basin, China, Xishanyao Fm. (Middle Jurassic) | Fig. 10; Jolivet et al., 2010; Heilbronn, 2014 |
| 31 | Yili Basin, China, Totounhe Fm. (Middle Jurassic) | Fig. 10 |
| 32 | Issyk-Kul Basin, Kyrgyzstan (Jurassic) | Fig. 10 |
| 33 | Sichuan Basin, China, Jialingjiang Fm (Triassic) | Zhang et al., 2015 |

B. Palaeozoic or Precambrian host rocks

- | | |
|--|---|
| 1 Parana Basin, SE Brazil, Teresina Fm (Permian) | Nomura et al., 2014 |
| 2 Appalachian Mountains, USA, Marcellus Fm (Devonian) | Fig. 11; Gilman & Metzger, 1967; Evans, 1995; Tobin et al., 1996; Gale et al., 2014; Aydin & Engelder, 2014 |
| 3 Appalachian Mountains, Quebec, Canada, Utica Shale Fm (Ordovician) | Séjourné et al., 2005; Chatellier, 2013 |
| 4 Barrandian Basin, Czech Republic (Lower Palaeozoic) | Suchy et al., 2002; Volk et al., 2002 |
| 5 Holy Cross Mountains, Poland (Devonian, Triassic) | Kowal-Linka, 2010; Rybak-Ostrowska et al., 2014 |
| 6 Junggar Basin, China, Lucaogou Fm (Upper Permian) | Jiao et al., 2007 |
| 7 Kalahari Desert, South Africa and Botswana, (Silurian-Devonian) | Watts, 1978 |
| 8 Australia, New South Wales, Murrumbidgee Fm (Devonian) | Barker et al., 2006 |

Preliminary
Version